7-2020

Implementation of Cholesteric Liquid Crystals in Fibrous Based Membranes

Ydana Yanell Virgen Gracia
The University of Texas Rio Grande Valley

IMPLEMENTATION OF CHOLESTERIC LIQUID CRYSTALS IN FIBROUS BASED MEMBRANES

A thesis

by

YDANA YANELL VIRGEN GRACIA

Submitted to the Graduate College of
The University of Texas Rio Grande Valley
In partial fulfillment of the requirements for the degree of

MASTER OF SCIENCE IN ENGINEERING

July 2020

Major Subject: Mechanical Engineering

IMPLEMENTATION OF CHOLESTERIC LIQUID CRYSTALS

IN FIBROUS BASED MEMBRANES

A thesis
by
YDANA YANELL VIRGEN GRACIA

COMMITTEE MEMBERS

Dr. Karen Lozano
Chair of Committee

Dr. Javier Ortega
Committee Member

Dr. Mircea Chipara
Committee Member

July 2020

ABSTRACT

Virgen Gracia, Ydana Yanell, Implementation of Cholesteric Liquid Crystals in Fibrous Based Membranes. Master of Science Engineering (MSE), July 2020, 77pp; 33 figures, 25 graphs, 15 tables, 63 references, and 81 titles.

The project consists of an investigation of optical sensors. On this project, the main focus was to implement materials that had properties such as thermochromism, piezochromism, and be able to detect volatile organic compounds with a color change response. The materials selected for this project were Cholesteric Liquid Crystals (CLCs) in different combinations and ratios. There were also four different methods using Forcespinning® technology to apply the CLCs into a polymer matrix; these were, In-Solution, Dip Coating, Coaxial Spinning, and Emulsion. The best results were given by Dip Coating, but the method with the best viable solution was Coaxial Spinning though it still needs further optimization.

DEDICATION

I dedicate this work to God, who always leads my way and protects my path. My parents, Lino and Zaed Virgen, my life's role models and the people I admire and respect the most, their love, support, and encouragement made me the person I'm today and reach the point at which I'm right now. My brothers, Lino and Gerardo Virgen, for whom I always try to give my best and my main motivation. My grandparents, whose stories and life paths teach me compassion, perseverance, and hard work. Lastly, I would like to dedicate this work to me, to the girl that started this career for others but stayed for herself. She that never gave up and decided to take the challenge of completing a higher degree. I'm proud of you. You made it!

ACKNOWLEDGMENTS

I would like to express my deepest appreciation to my supervisor, Dr. Karen Lozano for her guidance, support, and encouragement to pursue and complete this master's degree. I admire her life path and the support and care she has for her students, I'm really lucky to have been part of her team and work with her first hand.

I would like to thank Dr. Javier Ortega and Dr. Mircea Chipara for their support and counseling on this project. I would also like to thank Dr. Victoria Padilla, for all the time she spent explaining and helping on lab work, most importantly for the moral support through this project. Lastly, I would like to thank specially to my lab partners Dulce, Raul, Misael, and Carlos for sharing and accompanying me on this journey.

This project is supported by the NSF PREM award under grant No. DMR-1523577: UTRGV-UMN Partnership for Fostering Innovation by Bridging Excellence in Research and Student Success.

TABLE OF CONTENTS

Page

LIST OF TABLES

Page

LIST OF FIGURES

Page

LIST OF GRAPHS

Page

CHAPTER I

INTRODUCTION

Smart materials are those that exhibit a response in their properties due to it being excited. The response may be reversible and controlled to be used for specific applications. Cholesteric liquid crystals (CLCs) are smart materials that can be tuned to exhibit specific properties such as thermochromism, piezochromism, and others. This project analyzes the properties of different CLCs such as Cholesteryl Oleyl Carbonate (COC), Cholesteryl Nonanoate (CN), Cholesteryl Benzoate (CB), and Cholesteryl Chloride (CC). In this thesis, we develop nanofibers doped with CLCs in different combinations and ratios to analyze its performance for applications as optical sensors to detect changes in heat, pressure, and detection of volatile organic compound. As a matrix, three different polymers were implemented, Poly Vinyl Alcohol (PVA), Polystyrene (PS), and Polyethylene Oxide (PEO). In order to incorporate the CLCs into the polymeric matrix four methods were used; first, the in-solution method which incorporates CLCs into the spinning solution; second, the dip-coating method where nanofibers are dip-coated with CLCs leaving a layer of CLCs on top and the bottom of the membrane; third, the coaxial spinning method where the nanofibers were made by introducing CLCs inside a hollow fiber as it is being made; and finally the fourth method is the emulsion method, similar to the in-solution one as it is a mixture of polymer and CLCs, the important thing and what makes it

different from the in-solution method is that the polymer used is amphiphilic, this property solves the problem faced from the in-solution method by encapsulating the CLCs and therefore maintaining their optical properties. Results have shown that the incorporation of CLCs in a spinning solution is not a viable way to implement CLCs since the use of any kind of solvent, including water, will take away their optical properties. Therefore, the dip-coating was a more viable solution. By dip coating, CLCs had a matrix and their properties remained intact. The development of coaxial fibers was also pursued, a specially designed spinneret was 3D printed and used as prototype for these experiments. The emulsion method was the latest approach to the project, although it uses the same procedure as the in-solution method the difference lays upon the polymer chosen and its properties, this being Polyethylene Oxide (PEO) having amphiphilic properties. This property makes the PEO molecules arrange in a way that prevents water from mixing with the CLCs. To quantify the performance of these fibers, different characterization methods were implemented such as Scanning Electron Microscopy (SEM), Fourier-Transform Infrared Spectroscopy (FTIR), Dynamic Scanning Calorimetry (DSC), and Thermogravimetric Analyzer (TGA), on the material side. The results show that the in-solution method is not a viable method to handle CLCs because of the absence of the optical properties. The dip-coating method meets the requirements to detect changes in the environment using CLCs, although it isn't the most efficient or user friendly. The coaxial fibers showed to be the most viable method to handle CLCs while keeping the optical properties visible. Finally, the emulsion method showed promising results, but it still needs optimization to have better results in the visibility of their optical properties.

CHAPTER II

THEORETICAL BACKGROUND

Smart materials can be classified as materials which properties change according to the changes in their environment. Most often these changes have to do with temperature, pressure, pH, light, and electricity. There are many types of smart materials ranging from bulk polymers to films, chemicals, and more[1-3]. They are used for a diverse number of different applications from textiles to biochemistry and drug delivery [4-6]. Particularly there is one class of materials that can have a wide range of properties depending on its components and ratios, including thermochromism, piezochromism, and vapor sensing; these materials are called cholesteric liquid crystal (CLCs). Due to the versatility of this material, it can be implemented in a wide variety of industries such as food, textiles, medicine, automotive, and many more.

2.1 Optical Temperature Sensors

A temperature sensor is a device used to make the user aware of the rise or decrement in temperature. Temperature sensors have been used widely from simple uses as thermometers that display a measurement depending on the temperature of the body and/or surroundings to high-performance machinery for laboratories or industries that need an accurate reading of the temperature of a specific body or component, or a temperature reading of the surroundings. Temperature sensors can have very important applications to the point of saving someone's life

by accurately and promptly measuring anyone's body temperature. There are two main types of optical temperature sensors which response is presented as a color change, these are leuco dyes and liquid crystals, more specifically cholesteric liquid crystals, these materials can also be classified as thermochromic materials. [7]

2.1.1 Thermochromic Materials

Thermochromic materials are described as materials that change color depending on temperature. These materials can be divided into two categories: leuco dyes (LDs) and liquid crystals (LCs). These types of materials have been extensively investigated and used in a wide variety of applications from decorative applications like nail polishes or mood rings to thermodynamic applications and LCDs on the electronic approach. [2,3,8] Firstly, LDs are a type of dye in which its molecular configuration changes depending on different parameters, in this case, temperature. [9] Secondly, LCs are a state of matter falling between a liquid and a solid with particular properties, one of them is the thermochromism that some LCs show like cholesteric liquid crystals (CLCs). [10]

2.1.2 Leuco Dyes

Thermochromic leuco dyes are a type of dye that can change from colorless to color in the visible spectrum depending on either pH, light, or temperature. [9] Leuco dyes can either be reversible, meaning change back and forth from the leuco form (colorless state) to the visible wavelength of color or irreversible, where once the leuco form changes it stays in that chemical form. It is important to understand that the leuco form or "colorless state" doesn't mean that the material is transparent, but that the material shows its original color state, which changes once it is subjected to the external stimulus.

Looking at the thermochromic leuco dyes changing with temperature, both reversible and irreversible dyes have been used for different applications like thermal energy storage, fluorescent responses, and more. [8,11-14]

2.1.2.1 Leuco Dyes in Fibers

For the most part, leuco dyes in fibers were used as additives in an after the process for staining and create a thermochromic material using different processes like dip coating and ink printing. [15] Ilana Malherbe *et al.* were the first to successfully imbed leuco dyes into a fiber using electrospinning technology. [16]

2.2 Optical Pressure Sensors

A pressure sensor is a device used to make the user aware of the changes in pressure of anything for which the pressure is an important parameter. Stating that pressure is the force required to stop fluid or solid from expanding. There are several applications for which pressure sensors are used for simple everyday household items like a pressure cooker or a boiler to high maintenance, high-performance machinery such as airplanes, rockets, etc., the importance and demand of pressure sensing materials are increasing with new technology developing every day. There are several types of pressure sensors, although based on the focus of this thesis, the types of pressure sensors will be reduced to only optical sensors. More than types of optical sensors, are techniques used to see the changes in pressure, for the changes to be seen the key factor is the material used. There are two main materials used for optical sensing of pressure, these are a fiber Bragg grating and piezochromic materials such as liquid crystals, more specifically cholesteric liquid crystals (CLCs), some polymers and other materials like some perovskites and hydrocarbons. [17-21]

2.2.1 Piezochromic Materials

Piezochromic materials are materials that change color depending on the change of pressure applied to it. The response being a color change provides a user-friendly environment where take of action can be quick and reading of the response is understandable by almost anyone. Piezochromic materials have been implemented in some applications such as detection of cracking towards material failure using organometallic substances or polymers with metal complexes. [22,23] Some studies have also been done using liquid crystals as the piezochromic materials for applications such as sensing of pressure changes underwater. [24,25]

2.3 Volatile Organic Compound Sensors (VOC sensor)

A VOC can be described as chemicals characterized by their high vapor pressure at room temperature. The vapors produced by these chemicals are a result of their low boiling point, meaning that they evaporate at low temperatures; for example, benzene has a boiling point of -11°C. These chemicals are found in very common places such as paints, aerosols, cleaners, and disinfectants, etc. Because of the commonality of these chemicals, there is a really big concern about the amount of ppm (parts per million) of these chemicals in the air since the health consequences to the exposure can be very harmful. Mild health consequences from the exposure of VOCs can be headaches, irritation in the nose, due to inhalation of the chemicals or eye irritation by contact with the fumes and nausea. [26] Some mayor health consequences include damage to the liver, kidney, and nervous system leading to cancer. [27] The consequences may vary in each chemical due to the toxicity levels, it also depends a lot on the amount of time exposed to certain chemicals. Due to all these concerns about VOCs, there has been a lot of research done on how to prevent, detect, and deal with them. [28] As for this investigation, the research was focused on detecting VOCs using an optical sensor.

A VOC sensor is used to detect volatile organic compounds such as benzene, ethylene glycol, formaldehyde, methylene chloride, tetrachloroethylene, toluene to name a few of the most common. The focus is on optical sensors for this research the material chosen to detect these VOCs were CLCs. There has already been some research done using this material for this specific reason such as the work of Han *et al.* and Mujahid *et al.,* although the approach as to how they are implemented is different to increase the applications and uses. [29,30] The main point to approach the detection of VOCs using an optical sensor is because of the quick response and quick interpretation of the results, rather than having a reading that not everyone might be able to understand the meaning or interpret it.

Tang *et al*. and Winterbottom *et al*. used similar approaches and even some materials were the same to create the CLCs used to detect VOCs. Winterbottom's approach was the one chosen for this research to create the VOC CLCs and implement them into the work done. [31,32]

2.4 Liquid Crystals

LCs were the first liquid crystals discovered in 1888 by Friedrich Reinitzer, a German scientist. [33] LCs are a state of matter between liquid and solid, there are two main types of LCs Nematic and Smectic. [10,34] LCs have been used for many applications, other applications different from the ones previously discussed include alignment of carbon nanotubes, electronics, and many more. [35-38]

Within the nematic phase, there is the cholesteric nematic phase or chiral nematic phase, referred to as cholesteric liquid crystals (CLCs) or chiral liquid crystals. The CLCs are the ones that show the different properties targeted in this research; thermochromism, piezochromism,

and detection of VOCs. The chirality is the reason behind the thermochromism or color change in CLCs is due to the helical structure of the rod-like molecules. There is a direct relationship between the amplitude of the pitch in the helix and the wavelength emitted; a small pitch will result in a blue or violet color emission, while a large pitch results in a red or orange color emission.

2.4.1 Cholesteric Liquid Crystals

Cholesteric liquid crystals have been recently used as temperature sensors solely as the material in display, they are used in the food industry and medicine mostly for easy and promptly measure. [39,40]

Cholesteric liquid crystals are characterized by their helical pitch (p) as mentioned before. The wavelength emitted from the CLCs can be calculated by $\lambda=np$, where n is the mean refractive index of the CLCs. Cholesteric liquid crystals have been used for different types of applications mostly optical like mood rings, where the color changes due to temperature. Conversion of energy applications are also very common like LEDs, where the color changes due to the voltage applied to the LCs which changes their pitch. There are other types of applications being investigated in research for LCs like detection of fumes, D. Winterbottom *et al.* talks about the detection of organic vapors using liquid crystal films, the results show that sensing of the CLCs varies depending on the composition of the same, but that there is a clear determination of the fumes in the air. [32] Yang Han *et al*. reported an approach for CLCs to detect gases, specifically in this article CO2, by doping CLCs with chiral dopants which changed the helical twisting power (HTP) of the CLCs this approach introduced CLCs to the detection of inorganic compounds with ease. [29]

One of the main differences between LDs and CLCs is the transition of colors when increasing or decreasing temperature. LDs have an immediate change from one color to the other, while CLCs go through the whole spectrum from the coolest temperature point at which the color will turn red or orange to the hottest temperature point at which the color will reach a blue or violet tone.

2.5 Nanofibers

Nanofibers are fibers with diameters in the Nanoscale. The advantage that distinguishes the nanofibers from other types of materials is that apart from being able to be implemented in almost anything, the efficiency they provide by having the most available surface makes them the best candidate for some of the more complex applications.

Most often these fibers are done using polymers with specific properties depending on the applications. As of the last decade, there have been different types of methods created to produce this kind of fibers the most common one being electrospinning, where the solution from a syringe is extracted by an electric field that attracts the solution to the collector, one of the main advantages of electrospinning is the diameter of the nanofibers can be set with a minimum possibility of error. Electrospinning is good for making constant fibers, but on the production side, it lacks efficiency since the average amount made is about 0.1g in 1 hour. Although electrospinning is not very efficient in terms of the quantity of material in time. A more contemporary and efficient method to produce nanofibers is through Forcespinning® technology, created by Lozano *et al.* it is an innovative method that uses centrifugal forces rather than electrostatic ones to create nanofibers. Sarkar *et al*. state that Forcespinning® technology. [41] The solution can be made out of a mixture of polymer and solvent, used to dissolve the polymer or pure liquid state like polymer that is placed inside a spinneret which is placed in the middle of

the Forcespinning® machine. Once the parameters like rpm, time, etc. are set then the cycle starts the solution is ejected from the spinneret by centrifugal forces pulling the solution out of the spinneret. As the solution comes out of the spinneret the solvent evaporates and leaves a strand of solid polymer in the shape of a fiber, around the spinneret, are collectors which trap the fibers, depending on the type of polymer, time and rpm, the collectors create a mat of nanofibers which can be used for further experimentation and/or treatments. The nanoscale of the fibers using the Forcespinning® method is due to the diameter size of the needles at the end of the spinneret from which the solution comes out of, but the fact that the centrifugal forces are the ones responsible for the extraction of the fibers from the needles creates a very noticeable disadvantage against electrospinning which is the variation in diameter of the fibers with standard deviations greater than 5%. [21,22]

Diameter size might or might not be a deciding factor on the production of nanofibers for specific applications, therefore both electrospinning and Forcespinning® are used frequently for research purposes.

2.6 Liquid Crystals in Micro/Nanofibers

LCs have been recently introduced to nanofibers as the industry started to get more attention. The possibilities of applications and benefits of the combination of these materials are broad due to the property combinations of the same. One of the first methods used to implement both materials into one was coaxial electrospinning, which can be seen in different applications such as “electronic paper” where the liquid crystals were encapsulated inside transparent-hollow fibers and aligned using the melt spinning method as Masahiro Nakata *et al.* has shown. [44] Largerwall *et al*. also report that using coaxial electrospinning with liquid crystals affect the confinement effects of liquid crystals, although this technique is expected to provide new

functionalities to the fibers. [45] On a later article, Eva Enz and Jan Largerwall took the same approach as Largerwall on his first article, but used cholesteric liquid crystals in the core, is the first to use coaxial electrospinning with a cholesteric core which resulted in nonwoven fibers that changed color depending on temperature. [46] Similarly, Buyuktanir *et al*. used electrospinning technology to imbed CLCs into a fiber, the results showed several beads formed throughout the fiber where some CLCs got clogged. [47] The most recent approach to the incorporation of CLCs into fibers was realized by Yu Guan *et al.* by creating an emulsion of encapsulated CLCs and electrospinning that emulsion into a PVP fiber. [48,49] Barbero *et al*. explained in depth the twist transitions and effects of CLCs and forces generated by the confinement of the CLCs inside films or fibers. [50]

2.7 Liquid crystal/polymer dispersion

The dispersion of liquid crystals is also a topic of interest in this research as well as in many more. A lot of investigation has been done on this topic due to the versatility of using small particles and these particles containing a functional material such as LCs. A dispersion can also be called an emulsion, where particles of one substance are suspended in another one. [51] These emulsions have been used mostly for electro-optical applications such as Ahmad *et al.* studying amphiphilic polymer matrices showing important effects on the morphology and electro-optical properties of the material and Qi Yan *et al.* who reported a novel type of CLC particles resulting in reversible thermal responses and microstructure stability at high temperatures. [52,53] Although this research doesn't focus on the electro-optical properties of the CLCs, the type of materials, processing, and characterization methods used are important towards the goal of the investigation.

CHAPTER III

EXPERIMENTAL TECHNIQUES

3.1 Characterization/Instrumentation/Designing-Hardware

3.1.1 Differential Scanning Calorimetry (DSC)

The DSC is a thermo-analytical technique used to measure the variation of heat flow and phase transitions due to temperature. The principle of this technique is to measure the heat absorption or release of the same depending on the phase transition that the sample is undergoing, also known as an endothermic or exothermic reaction. The absorbance or release is then compared to that of the sample to measure the difference between both and give a reading of the sample's heat flow. As an example, as the temperature on solid sample increments it will go through a phase transition once it starts melting, the heat absorbed by the sample pan will be higher than the reference one because of the sample. On the contrary, when the temperature decreases and the sample crystallizes the absorbance of the sample pan would be lower than that of the reference pan because of the sample being crystallized and releasing heat faster than the pan itself. Although DSC is usually used for this purpose there are other observations that can be seen through the use of the DSC based on the physical changes of the sample due to temperature, like glass transition temperatures, impurities on the samples, or additives for specific purposes of the same. In order to get accurate processing the DSC sample's weight must be recorded and input in the program. The sample is then placed on a

sample holder and placed inside a closed chamber in a nitrogen environment to run the test. The sample is heated to a specific temperature, usually higher than the melting point but lower than the degradation point, then it is cooled to room temperature or lower if necessary. This cycle is repeated at least one more time to get rid of any impurities and have an accurate reading of the processability of the sample.

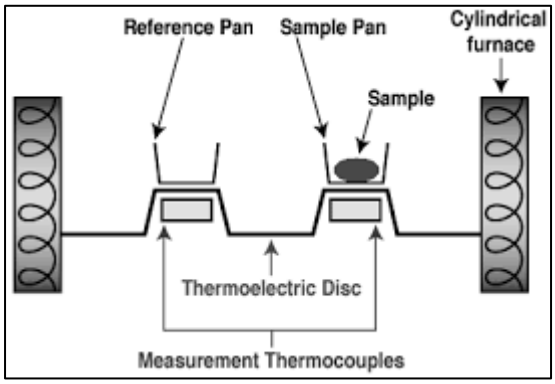

Fig. 01 Schematic of the interior of a TA Q100 Differential Calorimeter [58]

The resulting data for a DSC sample is a curve like the one shown above in figure 02; the curve is usually a heat flux vs temperature curve, but the curve can also be heat flux vs time. The curve shows exothermic reactions, if it is increasing or decreasing depends on the convention that the program has for each equipment. The curves are used to calculate the enthalpy for each transition; this is done by integrating the peak of any specified transition curve in the $\Delta H=KA$ equation, where ΔH is the enthalpy of transition, K is the calorimetry constant, and A is the area under the curve. The calorimetry constant may vary per instrument but it can be determined by analyzing a sample with known enthalpies of transition.

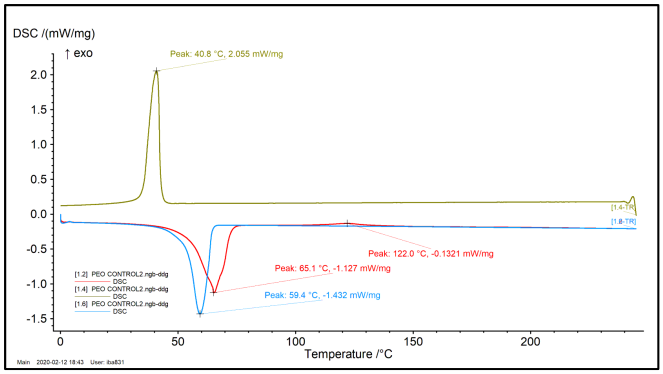

Fig. 02 Example of a DSC graph

3.1.2 Thermogravimetric Analyzer (TGA)

The TGA is a thermo-analytical technique used to measure the change of mass over time depending on temperature. The TGA can also be programmed to have a constant temperature to see the reaction of mass over time, it can also be programmed to control the temperature for a constant mass loss, depending on the application and type of characterization. For this research, the technique used for TGA is a dynamic thermogravimetric analysis, where the temperature is increased linearly. For this technique, the TGA sample is compared against a reference to measure the weight loss from the sample up to its degradation point to measure the thermal stability of the sample at a ranging temperature. The samples to characterize by the TGA are placed in a sample holder inside a furnace in a nitrogen environment. The sample is then heated to degradation point, meanwhile, the loss in mass is recorded and interpreted as a graph of Mass vs Temperature. The TGA is often used to look at the melting and degradation point of the sample as well as any impurities or different components that this may have as a kinetic thermogravimetric analysis.

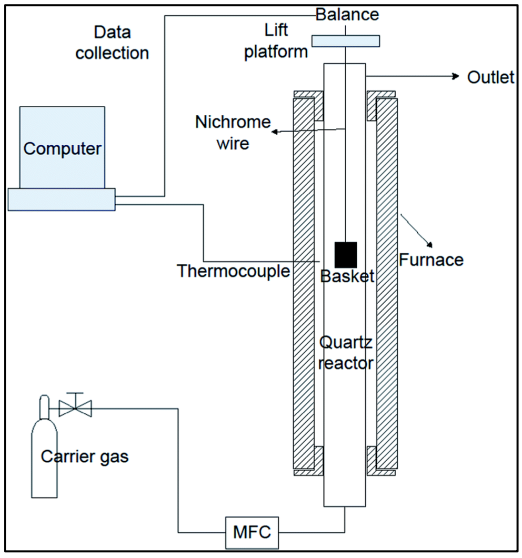

Fig. 03 Schematic of a Thermogravimetric Analyzer [59]

3.1.3 Forcespinning®

Forcespinning® is a method used to produce micro to nanoscale diameter fibers using centrifugal forces. The process of producing fibers using this method starts with a polymeric solution; this solution contains a polymer, solvent, and additives if required depending on the application desired. After the solution is in the desired state either homogeneous, emulsion, etc; it is added to the spinneret and collectors are placed around it. The machine is then turned on and, the spinneret starts rotating, note that the spinneret is in the middle of the machine with 30 - 18 gauge needles on the ends and surrounded by the collectors; as the spinneret rotates, the solution inside it gets pulled out by centrifugal forces while solvent gets evaporated leaving the polymer behind, therefore solidifying it in a fiber-like form and being collected by the collectors. The fiber mats collected can then be treated or used/characterized as needed. Forcespinning® technology is a cost-effective and efficient method for creating nano-sized fibers in great amounts to characterize or make a production of the same for industry applications.

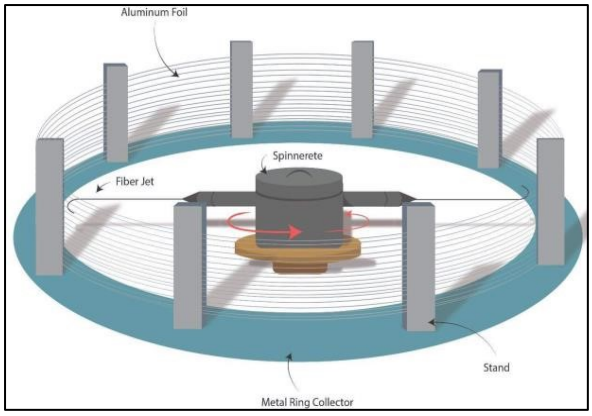

Fig. 04 Schematic of a Forcespinning® Cyclone

3.1.3.1 Coaxial Forcespinning®

Coaxial Forcespinning® is referred to as the Forcespinning® process of a fiber or a substance inside another fiber. To do coaxial Forcespinning® a special spinneret is required. The spinneret must have two chambers, to store the different materials; two needle holders, one inside the other, to have one needle inside another and both solutions are extruded from the spinneret one inside the other.

3.1.4 Fourier-Transform Infrared Spectroscopy (FTIR)

The FTIR is a spectroscopic technique used to determine the elemental composition and structure as well as the bonds between elements by the absorption or emission/transmittance of a material which is represented by an infrared spectrum. The basic theory states that each bond between elements has a unique absorption of light at wavelengths in the infrared spectra, about 700 nm to 1 mm.

The FTIR spectrum of an unknown sample is done by first using an interferometer that produces a signal/beam with many IR frequencies it also has a set of mirrors that help block the signal of certain wavelengths and allow others to pass through at different rates. Then the detector receives an interferogram, which is the raw data collected from the sample's absorbance and movement of the mirrors. After that, a second signal with different wavelengths of IR is shined trough the sample to produce a second set of data points to measure the absorbance by the sample from that signal. This process is repeated several times, taking a significantly short amount of time. The program using Fourier transformations analyzes the interferogram and works backward to infer how much was absorbed by the sample at each wavelength. Using Fourier transformations the program can convert the displacement of the mirrors in cm to the wavenumber in cm-1. The data is then compiled into a spectrum shown the absorbance of the sample at different wavelengths. This graph is then analyzed using known data to compare against the new sample and find out the bonds present in the material.

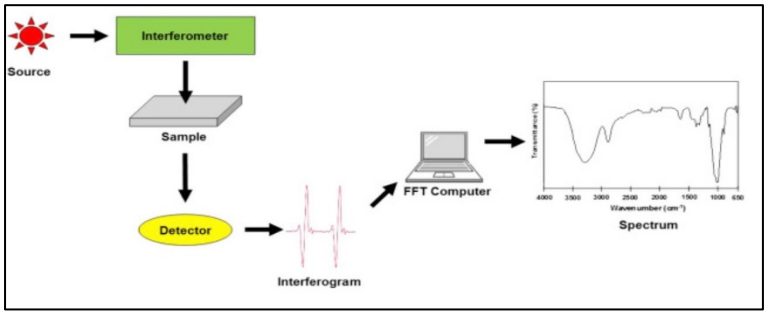

Fig. 05 Schematic of an FTIR system [60]

3.1.5 Scanning Electron Microscopy (SEM)

The scanning electron microscope is used to obtain the morphology of a sample by scanning the surface of it with a beam of electrons. It is important to discuss the sample preparation for the SEM because of its influence in the imaging. There is one important aspect of sample preparation, conductivity. Conductivity is important when preparing the samples, for a

better image resolution, a conductive material would perform better than one that is not. Therefore, when a sample is prepared for SEM the sample has adhered to the sample holder with carbon tape. On top of that, the sample itself needs to be conductive as well, for that reason, there are some methods used to achieve this goal. One is to sputter coat the sample, for this process gold is usually the material used because of its conductivity properties. Another way would be to place a silver dot on top of the sample to give some conductivity to the sample itself, this dot must make contact with the carbon tape and the sample at the same time. After sample preparation, the sample holder is placed in the vacuum chamber and the SEM is run. The process for imaging in the SEM starts by shooting an electron beam; after that, the ray goes into a condenser lens, which is used to converge the divergent beam. Then it goes into a limiting aperture to prevent the beam from scattering, an objective lens is then used to focus the beam into any part of the sample, while the scanning coils are used to move back and forward across the sample. On the side of the chamber is a detector that is used to detect any secondary, backscatter, x-ray, auger, and other electrons that are reflected or dispersed from the sample by the electron beam. The detection is then decoded and an image of the morphology of the sample is shown in the monitor. The images are then used for further analysis like element composition, fiber diameter distribution and other processes.

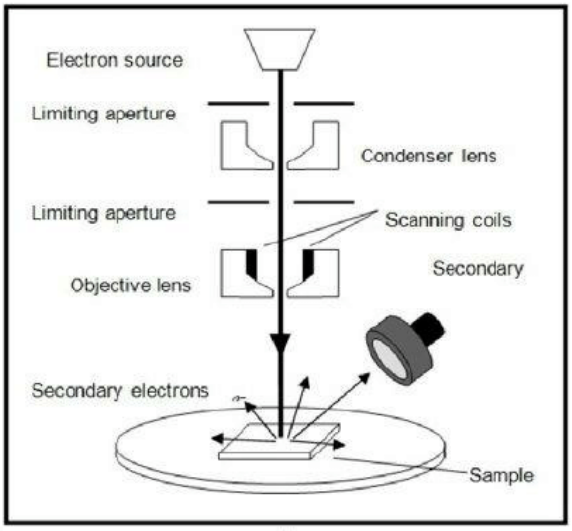

Fig. 06 Schematic of an SEM [61]

3.1.6 Tevo Tornado 3D Printer*

A 3D printing machine is used to create a 3D model off of computer-aided design (CAD). The most common materials used to 3D print are Polylactic Acid (PLA) and Acrylonitrile Butadiene Styrene (ABS). The way a 3D printer works is by extruding the polymer chosen in a rod-like structure, while the extruder moves in the x, y, and z-direction creating the 3D model.

Fig. 07 Image of a Tevo Tornado 3D Printer [62]

3.1.7 Optical Microscope

An optical microscope is used to maximize the imaging of an object or material. There are optical microscopes that can magnify an object from 10x to 1000x its optical sight. A simple optical microscope has two main components, light and magnification lens(es), like a magnifying glass which typically has a magnification of 5 to 10x. For more traditional optical microscopes, also known as compound microscopes, they have other features added to them like a stand, different magnification lenses, sample holders, hinges to bring sample closer or farthest depending on the focus point, etc. For more sophisticated microscopes things like a camera, a monitor, measurement programs, etc. are added as well. The way an optical microscope works starts by placing the sample in a sample holder, then the light, either natural or from a light bulb pass through the sample straight up to the magnifying lens(es) up to the eyepiece lens. The magnifying lenses and light are still the two main components for any optical microscope, as the light passes through the lenses the image gets distorted in a way that it appears to be bigger. The magnifying lenses and eyepiece lens have different depth depending on the magnification desired and they may also be composed of a series of different lenses.

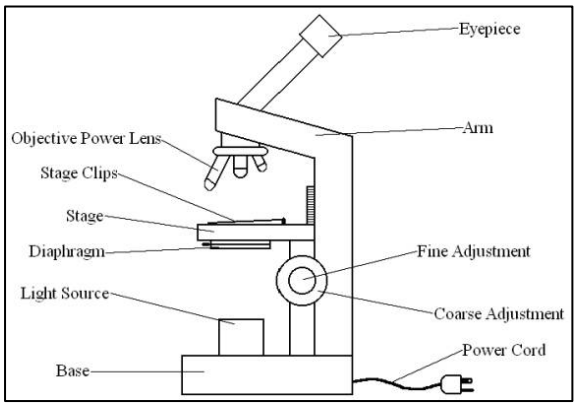

Fig. 08 Schematic of an Optical Microscope [63]

3.2 Characterization/Instrumentation/Designing-Software

3.2.1 Solidworks

Solidworks is a computer-aided design program used to create 3D models to be displayed or printed for a better understanding of the design created. Solidworks uses a parametric feature-based approach to create the designs, this allows for the program to use parametric geometries and create complex designs with parametric numbers to specify the length, diameter, or any other quantitative number for a certain measurement of the parts. Solidworks also allows the user to set parts within the designs and specify its position regardless of the changes later made to the rest of the design. For better organization of the design, Solidworks allow for parts to be made separately and then put together in an assemble, so that updating or modifying a part is easier.

3.2.2 ImageJ

ImageJ is an image processing program from Java mostly used to edit, analyze and process images by calculating areas with pixel value, measuring distances or angles, identifying and creating different parameters for the specific purposes of using the program.

CHAPTER IV

EXPERIMENTAL PROCEDURES

4.1 Materials

Cholesteryl Oleyl Carbonate (COC), Cholesteryl Nonaoate (CN) also known as Cholesteryl Pelargonate (CP), Cholesteryl Benzoate (CB), Cholesteryl Chloride (CC), Polyvinyl Alcohol (PVA), Polystyrene (PS), Polyethylene Oxide (PEO), Tetrahydrofuran (THF), Toluene, Ethylene Glycol.

4.1.1 Preparation of CLCs

To prepare a solution of temperature-sensitive CLCs in the range of 17-23°C, 65% COC, 25% CN and 10% CB were added into a vial and heated up to melting temperature and clear looking solution. Finally, the end product is left to cool.

Similarly, for a solution of pressure-sensitive CLCs, 38% COC, 38% CN, and 25% CC are added in a vial and heated up to melting temperature and clear looking solution. The final product is left to cool. Both preparations for temperature and pressure-sensitive CLCs were based on the procedure done by Katz, which is mostly based on the work done by Brown and Elser, as well as Patch *et al.* [54-57]

For the VOC sensitive CLCs, the solution was prepared by adding 19% (v/v) of a stock solution of 1.0% (w/v) CC in THF and 81% (v/v) of a stock solution of 1.0% (w/v) CN in THF. This procedure is based off of the work done by D.A. Winterbottom *et al.* [32]

4.1.2 Preparation of Polymer Solutions

PVA was chosen because it is a semi-crystalline material and is a fairly easy material to work within the process of fibers. PVA solution was prepared by adding 1.5g of PVA to 8 mL of water. The solution was then placed in an oil bath for two hours, removed, and placed in a stirring plate until Forcespinning® was started or further preparation was initiated.

PS was chosen because it is an amorphous material and it has very good optical properties. PS solution was prepared by adding 0.7g PS to 10 mL Toluene. Afterward, the solution was placed in an oil bath for 1 hour, removed, and placed in a stirring plate until Forcespinning® was started or further preparation was initiated.

PEO was chosen due to its amphiphilic properties, which give it a double affinity towards water, this way it was believed that PEO would act as a capsule containing the CLCs and separating them from the water. PEO solution was prepared by adding 10% PEO with a molecular weight of 600,000 in water. The solution was stirred by hand and then placed in an oil bath for 15 min., it was then removed and placed in a stirring plate until Forcespinning® was started or further preparation was initiated.

4.2 In-Solution Procedure

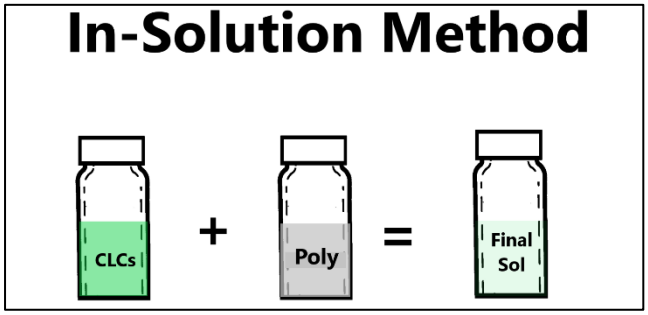

Fig. 09 In-Solution method schematic of the procedure

To prepare in-solution temperature and pressure CLCs it is necessary to make the polymer and CLCs' solution separate. The CLCs' solution is then added to the polymer solution by heating it to a liquid state. Using a glass rod both solutions are mechanically stirred, they are then placed in an oil bath at 75°C for 1 hour, with the exception of PEO which is left in an oil bath for 15 minutes. The solution is then removed from the oil bath and placed in a stirring plate until it is ready to be forcespun.

For VOC in-solution CLCs, the polymer is added to the already made VOC CLCs solution. The amount of polymer is dependent on the viscous properties of the material and its molecular weight. After the addition of polymer into CLCs, the solution is placed in an oil bath for 1 hour. The solution is then removed and placed in a stirring plate until it is ready to be forcespun.

4.3 Dip Coating Procedure

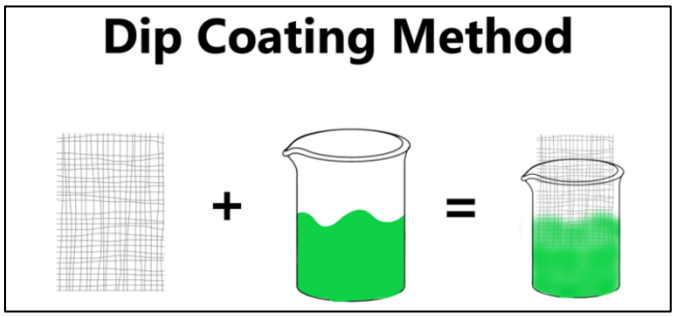

Fig. 10 Dip Coating method schematic of the procedure

The coating of nanofiber mats with temperature and pressure CLCs is done by first creating a mat of nanofibers using Forcesppining technology. The mat is then submerged in a CLC bath for it to get the mat coated. The excess CLCs are removed and the mat is placed inside a plastic bag to be handle since these CLCs do not dry and leave some residue when touched.

The coating of nanofiber mats with VOC CLCs is done by placing the mat on a glass platform and start coating the fiber by small drops of the CLCs until everything is covered, it is then left to dry.

4.4 Forcespinning® Procedure

Fig. 11 Forcespinning® Technology Cyclone 1000

The Forcespinning® procedure is done by setting up the spinneret. To set up the spinneret, the spinneret is placed in the spinneret holder and adjusted to the machine so that it only moves in a rotating direction and not up and down. The solution already ready to be spun is then injected into the spinneret and two needles of certain gage, depending on the solution, are placed at both ends of the spinneret. After that, the doors are closed and the set up of the run is specified depending on the solution to be spun.

For PVA the run is set at 6400 rpm for 5 minutes, ideally, the humidity should be between 35% and 40% so the amount of fibers is higher. For PS the run is set at 6000 rpm for 5

minutes. Finally, for PEO the run is set at 7000 rpm for 5 minutes. All variations of solutions containing these polymers were run at around the same parameters.

After each run, the fibers were collected using a collector. The fibers were then placed in aluminum foil to be used later on for characterization or further procedures.

4.5 Coaxial Spinning Procedure

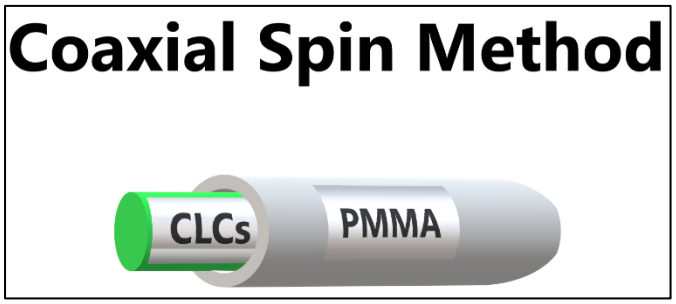

Fig. 12 Coaxial Spinning method schematic of the procedure

The coaxial spinning is done the same way as the Forcespinning® method, the only difference is the design of the spinneret to get the structure desired in the fibers. The coaxial structure of the fibers is believed to give better results for the optical properties as well as take care of the handling problem due to the viscous nature of the CLCs. The spinneret used to create these coaxial fibers has two chambers, one inside of the other one. These chambers are then connected to a needle, 30 gauge for the inner one, and 18 gauge for the outer one. One important detail about the placing of the needle is that the inner one, 30 gauge, has to be larger than the outer one, 18 gauge, to prevent clogging of the same. This procedure is used to create the structure of the coaxial fibers by introducing temperature or pressure CLCs inside a core-shell made of a designated polymer, in this case, Polystyrene. Polystyrene was chosen as the designated polymer for the core-shell of the coaxial fibers because it is an amorphous polymer, therefore it lets the optical properties of the CLCs to be visible.

4.5.1 Solid Works

The following images show the different components from original drawings to the current design.

4.5.1.1 First and Second Design

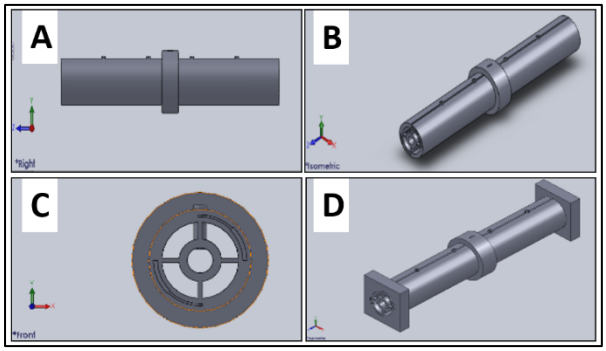

Fig. 13 First and Second design views of the coaxial spinneret shaft

These figures are the first designs of the shaft for the new coaxial spinneret, at this point, there are already two chambers in the design, one inside the other one. The chambers have two connections each, of which are connected to the upper surface of the outer chamber. These connections are used to inject the desired solutions, the centermost holes connect to the inner chamber while the farthest holes connect to the outer chamber. On figure 13D, the square design was added to add a connection for the outer needle. This connection was not possible using this design due to the width of the outermost chamber, which was broader than the fixture for the outer needle.

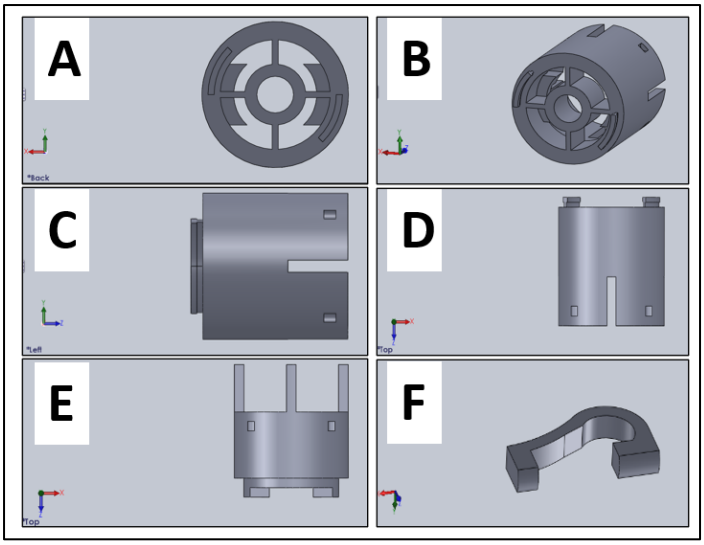

Fig.14 Second design views of the coaxial spinneret attachments and clip

In order to fix the outer needle to the chamber, an attachment was necessary, the figures above show the drawings of the first attachments. On figure 14C the center tube protrudes out of the cylinder to get the fixture of the needle attached and screwed on to it. Figure 14C and figure 14E assemble perfectly to one another, although because of the size of these attachments, 3D printing them was a challenge and for them to remain together four clamps were necessary, figure 14F. Even with all these fixes, a problem remains, the single rods protruding out of figure 14E were easily broken and needed a higher resolution for 3D printing them correctly. Therefore, another design was needed.

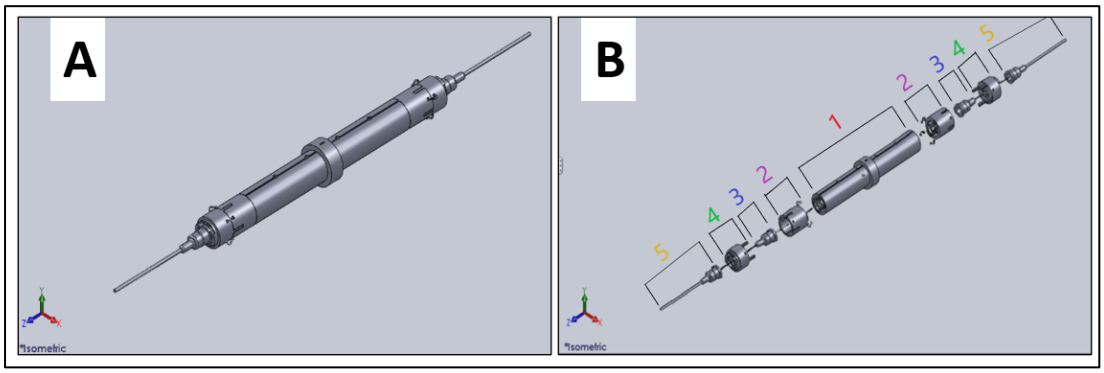

Fig. 15 Rendering of Second design for coaxial spinneret

Figure 15 above shows an exploded view of all the components that would have been added to the spinneret. This design used the attachments previously explained and as the previous explanation, this design was reevaluated. Part 1 is the shaft of the spinneret, where the two chambers are located. Parts 2 are the first attachments for 30 gauge needles. Parts 3 are a representation of the 30 gauge needles. Parts 4 are the attachments for the 18 gauge needles and finally, parts 5 are a representation of the 18 gauge needles.

4.5.1.2 Third Design

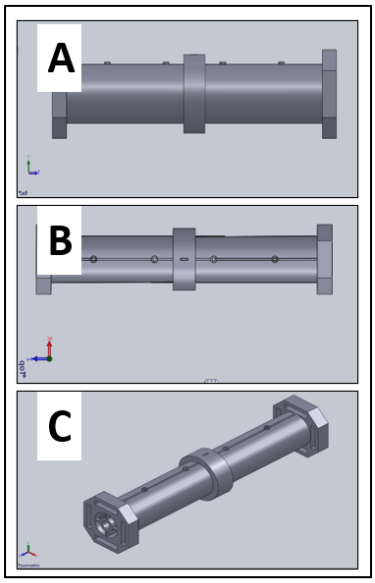

Fig. 16 Third design of coaxial spinneret shaft

Compared to the previous figures 13A-D of the shaft for the new coaxial spinneret, this design was changed to an octagon figure at the ends to make a rounder structure but still have space for the clip holes used to keep the attachment attached to the shaft. Another change made to the shaft was to the middle part protruding from the shaft, the middle part was cut in the bottom for the shaft to not rotate and keep still in the spinneret.

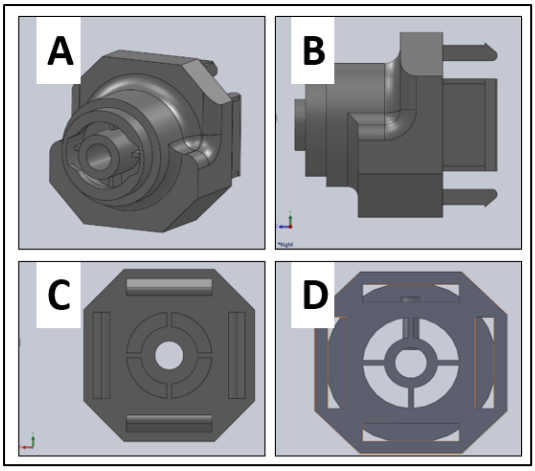

Fig. 17 Third design of coaxial spinneret attachment

The figures above show the new attachment design, the main changes were done to the design are the fact that there is only one piece, not two as in the previous design, combining parts shown in figure 14C and 14E. This change also resulted in placing the 30 gage needle directly into the inner chamber, which is more efficient and there is less probability for the two solutions to mix. The other change is in the clips already added to the design in a way that they serve as a fixture to attach the attachment to the shaft and keep them together by also clipping once inserted. This design works a lot better than the previous one mainly due to the size and printability of the part.

The previously discussed attachment also helped compact the part as a whole, which helped with the aerodynamics as specified in the original design of the spinneret.

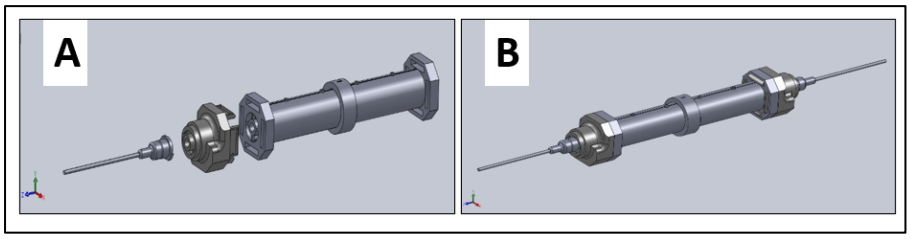

Fig. 18 Third design rendering of the coaxial spinneret

Figure 19A shows how the new part looks after 3D printing, as seen in the pictures the bottom and upper part of the original spinneret are still part of the design. Picture 19D shows how the needle will look like after the setup is done.

Now to set up the coaxial spinning to run fibers, the first thing was to introduce the CLCs in the inner chamber, then the 30 gauge needles were placed in their respective place at each end of the shaft, then the adaptors were connected. The PS solution was then added to the outer chamber and the 18 gauge needles were then placed at the end of each adaptor over each 30 gauge needle. The spinneret was then adjusted to the spinneret holder inside the Forcespinning® machine. The machine was then closed and the setup of the run was edited. For the coaxial spinning run set up, it was necessary to make the runs at a slower RPMs between 4000 and 5000 due to some complications with the parts. The time was also reduced to 1 minute, although the needles were not changed as often as with a normal Forcespinning® technique. The fiber samples were then collected in a normal way with a fiber collector and placed in aluminum foil.

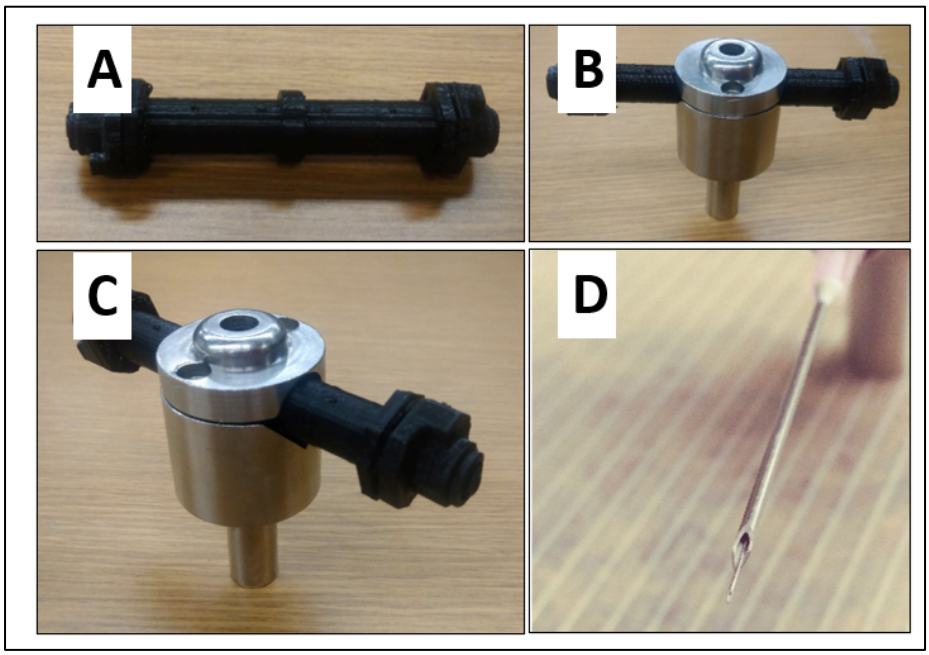

Fig. 19 3D printed coaxial spinneret

4.6 Emulsion Procedure

An emulsion is a mixture of two or more substances where at least two of them are immiscible to each other, the term “emulsion” is used specifically when two or more liquids are the ones interacting in the mixture. A clear example of an emulsion is oil in water or water in oil depending on the preferred dispersive medium; the water and oil repel each other which prevents them from forming a homogeneous solution. Therefore, on that note, it was proposed to create an emulsion solution of CLCs with a solution of PEO in water. This solution was believed to create a self-coaxial fiber, where the droplets of CLCs would get encapsulated by the PEO, due to its amphiphilic properties

A 20% CLC/PEO solution is combined by the mechanical stirring of a homogenizer at level 3 for 3 minutes. The solution is then placed in an oil bath for 15 minutes, it is then removed and left stirring overnight. The solution will then have a continuous medium of water with CLC droplets dispersed along with the medium and encapsulated by PEO.

4.7 Characterization

4.7.1 DSC

Fig. 20 Netzsch DSC 214 Polyma

The DSC was used to analyze the samples made in this project and their components. The DSC runs may show important endothermic or exothermic reactions, meaning fluctuations in the absorbance or releasing of energy presented by heat. The explanation of these behaviors may lead to the configuration and manufacturing processes of the material tested, from these discoveries the user can make educated decisions towards the performance and uses of the material.

Taking into account the variety of samples and their components being tested in this project it was important to analyze the parameters necessary for each sample and because of time restrictions, if possible, it was preferable if the runs were able to take the least amount as possible as well as having several samples use the same baseline, meaning that the samples would run with the same parameters in each run. Firstly, TGA analysis was done to all the samples, it helped to have more information about them as well as to have important information to set the parameters necessary for the DSC runs like melting temperature(Tm), degradation temperature(Td) and glass transition temperature(Tg). To set the parameters for a DSC run it is important to set the starting temperature lower than that of the Tg so that the user can identify that specific point through the run. For the end temperature of the run, it is important to set it to be as farther as possible from the Td, at least 30-50°C lower if possible, but it shouldn't be lower or interfering with the Tm since that point is also important for the data collected.

To start the actual testing of the samples, as stated before it is important to set the parameters at which the DSC will run. Each sample is composed of two components, a polymer, and a CLC unless the ones tested are the components by themselves. The components were tested by TGA by themselves as well as the composed samples, Tm, Td, and Tg were recorded from the TGA data and compared with one another to set the parameters that covered most, if not

all the samples. Since there are solid and liquid samples, their baseline had to be different based on the fact that the sample holder needed for each type of sample had to be different depending on the state of the sample. The standard sample holder would be a closed crucible, which would be used to hold solid non-corrosive samples inside. The crucible used for liquid samples has a hole in the lid of the crucible for gases to escape, because of this hole the reaction of the crucible to the environment would be different and therefore the baseline would behave differently from the one made by the standard one.

After analyzing all the data from each sample it was decided that based on the similarity of the parameters from TGA analysis PS and PEO solid samples would be tested with the same baseline, PVA solid samples having a lower Tm and Td would run at a different baseline as well and finally the last different baseline would be for the CLCs since, as explained before, the samples would be placed in a different type of sample holder.

In order to prepare a sample to be tested by the DSC, it is necessary to measure 10mg of the sample to be tested. The 10mg sample is then place in the base or pan of a DSC crucible, in this case, the crucible was chosen to be made of aluminum since it can withstand the highest temperature at which the sample will be subjected, the lid of the crucible (the lid's design changes depending on the state of the sample, standard-closed lid for solids or lid with a hole for liquids) is then punched in and hermetically closed using a press that has die the size of the crucible. After the crucible is ready, it is then placed beside an empty control crucible. Using the program Proteus a baseline is needed for each set of parameters, the baseline is done with an empty crucible. This baseline is used to record the behavior of the crucible with the environment based on the parameters stated. The baseline would then be used in runs made by each sample.

The first baseline that would be used to test PS and PEO samples starts with a 0°C temperature, the temperature remains the same for 5 min. to stabilize the environment and get an accurate reading. The temperature then rises 5°C/min. up to 280°C, it then stays at that temperature for 15 min. to stabilize the environment. The temperature then decreases at 5°C/min. down to 0°C, it again remains at that temperature for 15 min. Finally, the temperature rises again 5°C/min. up to 280°C and that is where the run ends. The whole process takes about 3 hours.

The second baseline used for PVA solid samples followed the same procedure as the first one, although for this baseline the rising top temperature was to 245°C. The starting temperature, time at which temperatures remained, and the ratio at which temperatures rose or decreased remained the same. The change of the rising top temperature was necessary because of the degradation temperature of PVA which is about 310°C, considering 280°C to be very close to that temperature.

The third and final baseline was used for liquid samples; liquid crystals control samples and liquid crystal-dip coated samples of all compositions. The parameters of the baseline remained all the same, temperatures, times, and ratios. The one thing that changed as discussed previously was the crucible, since this has a hole on the lid, because of this change the environmental conditions would have a drastic change compared to the first baseline.

4.7.2 TGA

Fig. 21 Netzsch TG 209 Tarsus

The TGA was used to analyze the changes of each sample by the increment of temperature. To run a TGA test it is necessary to measure the sample desired to be about 10 mg. The sample is then placed in an alumina crucible and placed inside the TGA to be processed. The TGA program Proteus is then set up to perform a run starting at 25°C up to 600°C by increments of 7°C/minute for a more accurate reading since most of the samples have 3 or more components. After the run is completed, the crucible needs to be cleaned up to place a new sample. To clean up the crucible the procedure starts by removing any loose residue that is left in the crucible by passing a swap inside it, the crucible is then placed in a vial with ethanol and put inside a sonicator bath for 1 minute, the sample is then removed from the bath and cleaned again with the swap to remove any loose residue that might have been detached from the crucible. The final step is to heat the crucible with a torch to the point where any residue attached to the crucible is degraded, after that the swap is again passed inside the crucible and finally it can be used again.

4.7.3 FTIR

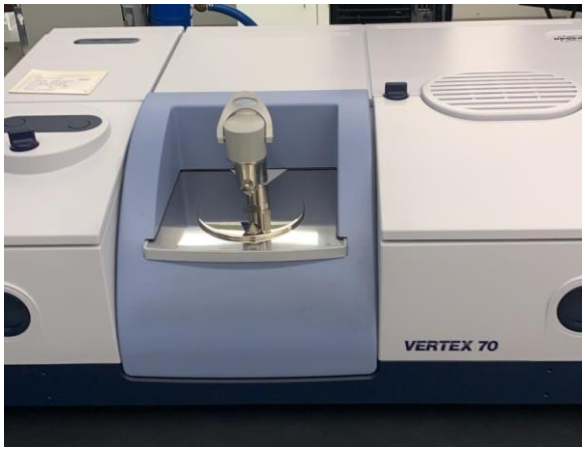

Fig. 22 Bruker Vertex 70 FTIR Equipment

The FTIR was used to identify the components of each sample by their transmissivity. To prepare solid membrane samples for the FTIR a small amount of the sample is cut and use as it is, a liquid sample needs a special holder so that the FTIR does not detect it and only reads the sample's infrared (IR) spectra. For a powder sample it is necessary to mix the sample with Potassium Bromide (KBr) and form a pellet by compressive pressure, KBr is "invisible" to the IR spectra and therefore the only spectra shown by the FTIR is that of the sample. Although there are certain complications with KBr since it is very hygroscopic, the sample would need to be prepared and tested on the spot for the pellet to not absorb too much humidity.

4.7.4 Optical Microscope

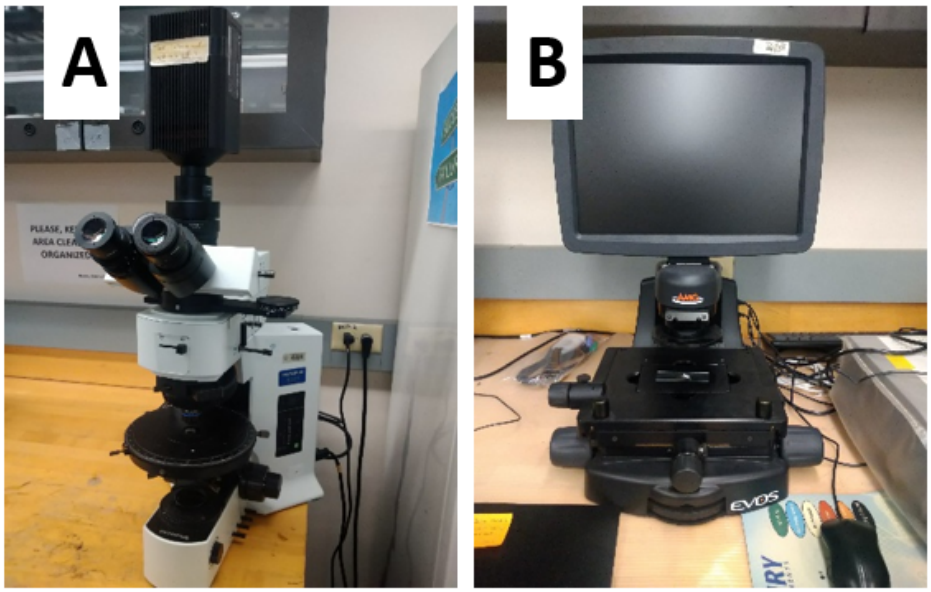

Fig. 23 Optical Microscopes (A) Olympus, (B)EVOS

The optical microscope was used to take images of the CLC solutions, pictures of the emulsion samples, as well as preliminary images of the coaxial fibers. There were two optical microscopes used, the Olympus and the EVOS. The first one was used to take images of the CLC solutions and the preliminary images of the coaxial fibers. The second one was used to take pictures of the emulsion solutions before and after oven treatment.

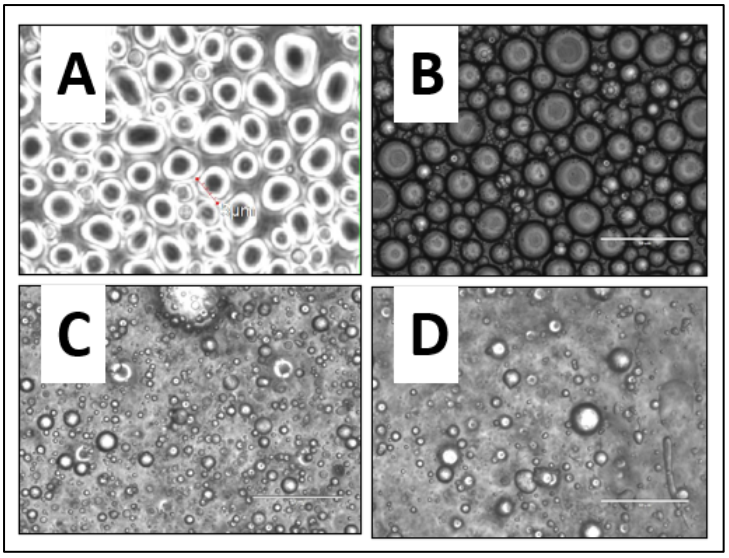

Fig. 24 Emulsion solutions through an optical microscope

PEO with Pressure CLCs mixture shows the encapsulation of CLCs by PEO in a water medium. The mixtures were prepared as explained above. After getting samples for characterization, they were then placed in an oven at 80 C for 24 hours to evaporate the water in the solution. Using Image J software, the diameters of the drops before oven treatment figures 24A, 24B were measured to be between 5 to 10 um. After oven images, figures 24C, 24D show no changes in the mixture. RAMAN was used to identify the components in the mixture, which will be discussed in the next section.

4.7.5 SEM

The SEM was used to analyze the topography of some of the samples. Wet samples, like the dip-coating ones were not able to be characterized by the SEM because of the vacuum produced in the SEM which if a wet sample was to be exposed to, would damage the equipment. The SEM was used to take images of the samples to measure the diameter of the fibers and see the cross-sectional area in coaxial fibers.

Fig. 25 Σigma VP-ZESS Scanning Electron Microscope

4.7.6 Image J

Image J was used to analyze SEM and EVOS optical microscope images. All images were analyzed to measure the diameter of the fibers and emulsion process before and after oven treatment, respectively for different samples. The diameter was measured by using the pixel value of the image in comparison to the magnification at which the image was taken.

CHAPTER V

RESULTS AND DISCUSSIONS

5.1 In-Solution Characterization

5.1.1 Resulting Fibers

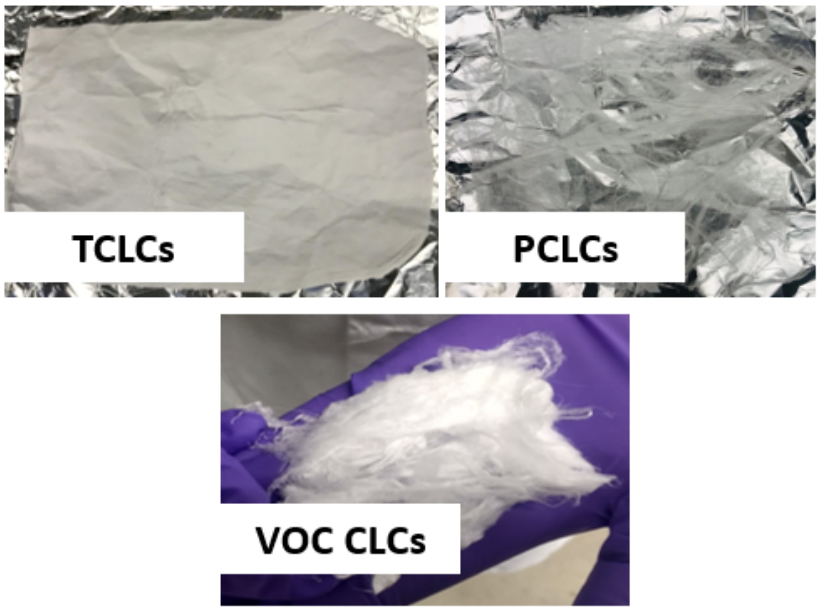

Fig. 26 Resulting fibers using In-Solution method

As can be seen in the pictures above, the fiber after being forcespun doesn't show any color. Even after applying temperature, pressure, or exposing them to VOCs, respectively the fibers remained the same. After further experiments, it was seen that any solvents including water take away the optical properties of the CLCs, although after evaporation of the solvents they can come back to their original state and show the optical properties. The problem with this

method is the combination of the solvent with the polymer, the solvent takes away the properties of the CLCs and the addition of the polymer prevents the CLCs from going back to their original state. Therefore, the resulting fibers come out to be as how the fibers from only the polymeric solution would look like.

PEO on the other hand, in theory can show color in the fibers even though the PEO solution has water in it. The reason for these results is the amphiphilic property of PEO, which makes the PEO act as a layer between the water and the CLCs creating capsules.

5.1.2 Fiber Diameter

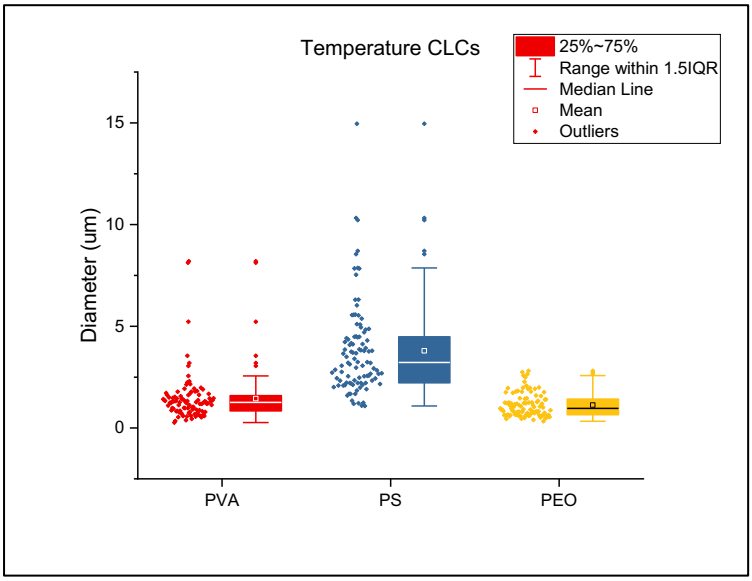

Graph 01 Diameter distribution of In-Solution fibers for TCLCs

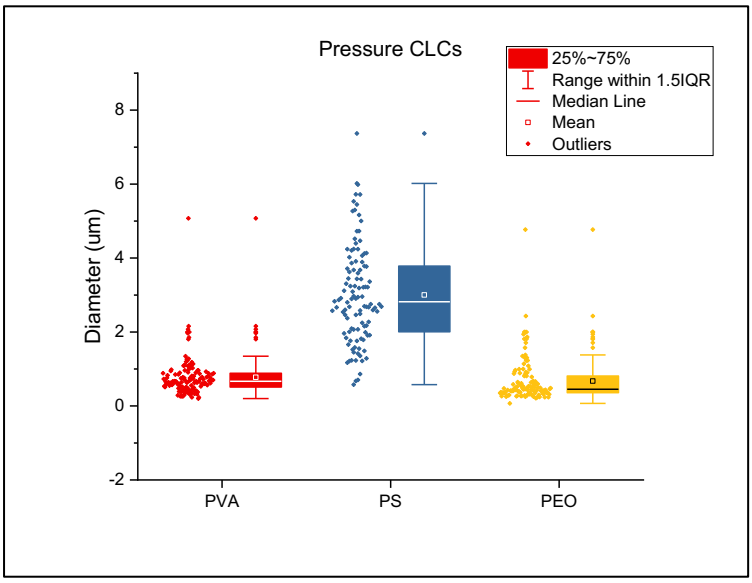

Graph 02 Diameter distribution of In-Solution fibers for PCLCs

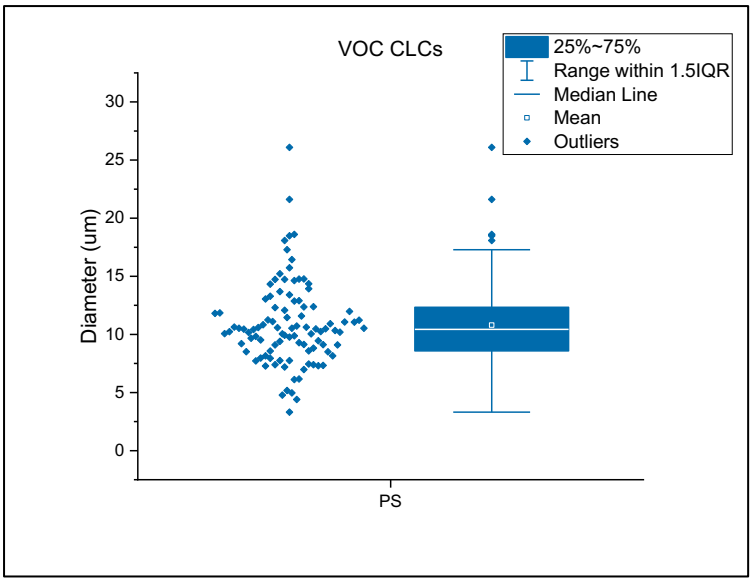

Graph 03 Diameter distribution of In-Solution fibers for VOC CLCs

The graphs shown above show the distribution of diameter in the fibers of PVA, PS, and PEO with Temperature CLCs and Pressure CLCs. The data shows that fibers with TCLCs have an average diameter of about less than 5 um, while fibers with PCLCs have a diameter of about less than 2 um in general.

5.2 Dip Coating Characterization

5.2.1 Resulting Fibers

Fig. 27 Dip coated fibers

The fibers shown above represent how any fibers would look like after being dip-coated with the respective CLCs. As can be seen, dip coating the fibers gives the CLCs the matrix needed as well as maintaining their optical properties, but the problem of handling and having to add a film or something to keep the CLCs encapsulated remains. Therefore, although as it does work for the practical application of the CLCs, it can still be improved.

5.3 Coaxial Forcespinning® Characterization

5.3.1 Resulting Fibers

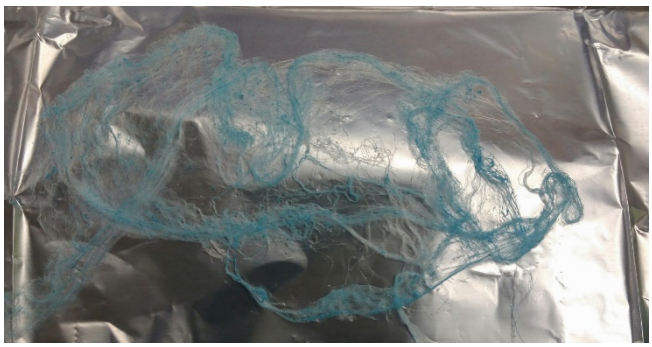

Fig. 28 Coaxially spun fibers

To test the 3D printed spinneret, a coaxial fiber with blue PEO inside a fiber of PS was ran. As can be seen in the picture above, the fibers created showed the blue color of the PEO

fiber. Although at this point it wasn't certain that the fiber was coaxial, it was proved that the 3D printed spinneret did work as expected.

5.3.2 Optical Microscope

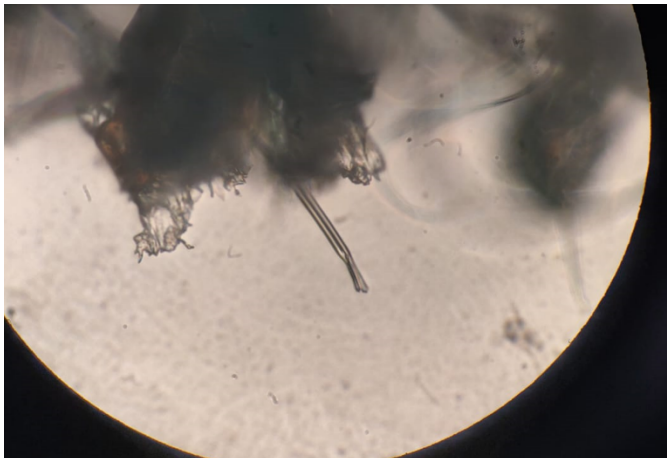

Fig. 29 Microscope image of coaxial fibers

The picture shown above was a characterization done to the fiber in figure 29, in the image it can be seen how a string passes through the middle of a fiber. Although there is still no certainty about what material is which and that a possibility remains of the string being behind the fiber, this image is a good indicator of what was expected from the fibers.

5.4 Emulsion Characterization

The emulsion method as discussed previously is similar to the In-Solution method in the way of the components used and how they are mixed. Both polymer and CLCs are combined in one solution, then mixed and finally spun. The main difference is the reaction of the polymer towards the CLCs since the polymer used for this method is Polyethylene Oxide and this material has the amphiphilic property preventing the solvent, in this case, water to be in contact with the CLCs by creating a PEO layer around bits of the CLCs solution making capsules of CLCs, which will be later shown and discussed. Although this method seems very favorable

there is still one main problem. For this process the size of the capsules compared to the size of the fibers has to be optimum. The capsules need to fit within the diameter of the fibers and hold their surface tension to show the color seen in the solution.

5.4.1 Resulting Fiber

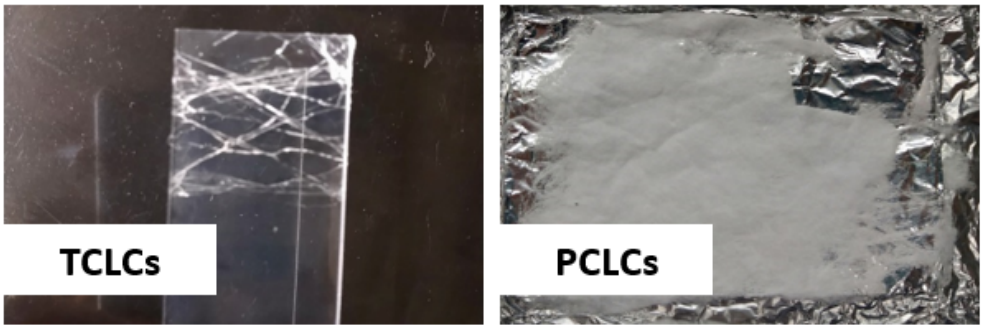

Fig. 30 Fibers using the emulsion method

The pictures above show the resulting fibers using the emulsion method. Here it can be seen that the fibers look white, meaning that they might have probably lost their optical properties. To confirm this theory further analysis is required.

5.4.2 Optical Microscope

5.4.2.1 Emulsion Solution

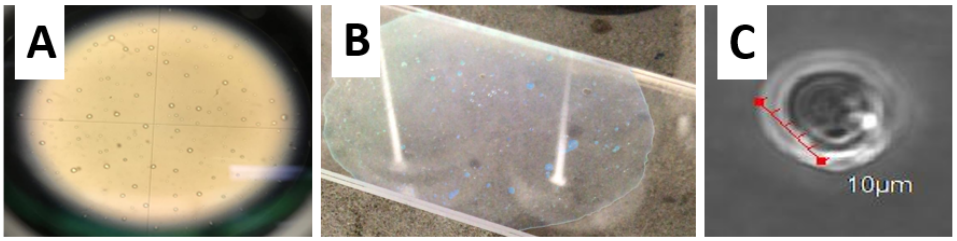

Fig. 31 Emulsion solute on images

The images shown above are from the emulsion solution before being spun. Figure 31A shows that there are drops dispersed in the solution. Figure 31B is a picture taken at the glass slide with the emulsion solution, this image shows that the optical properties of the CLCs are still

present. Finally, figure 31C is an image of one of the drops in the solution, it shows a diameter of about 10 um, this measurement is important to better understand the mechanical and dynamic variants that the droplet might have once it is spun, passing through a needle of 30 gage which is roughly about 0.25 mm, and expected to hold on to a fiber in the nano range. From these results, it was seen that for the droplets to hold on to the fibers, there had to be some changes done. It was either decrease the size of the droplets or increase the size of the fibers. Since the diameter size can't be stated in the Forcespinning® machine, then the other solution would be to reduce the size of the droplets, for this it was decided to heat the solution before spinning it at 80°C for 24 hours.

5.4.2.2 Diameter distribution

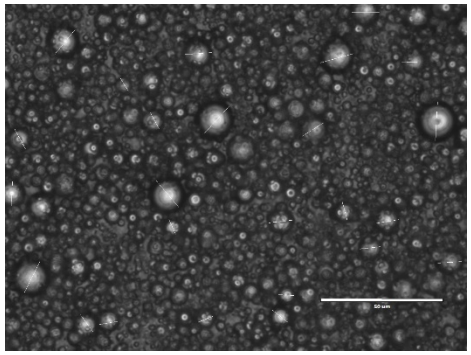

Fig. 32 Emulsion solution before oven treatment

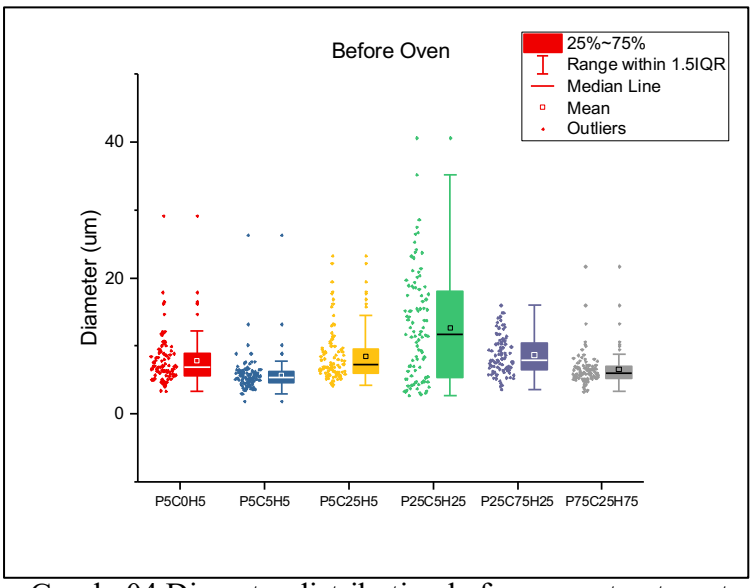

Graph. 04 Diameter distribution before oven treatment

To get measurements of the droplets from the solution the EVOS optical microscope was used. After the images were analyzed using Image J, it was determined that the average diameter before the oven was at around 10 um for all the different recipes tested.

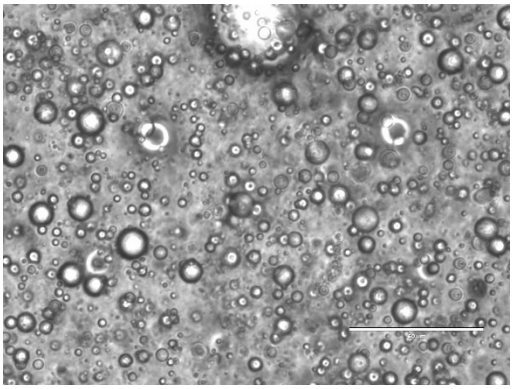
Fig. 33 Emulsion solution before oven treatment

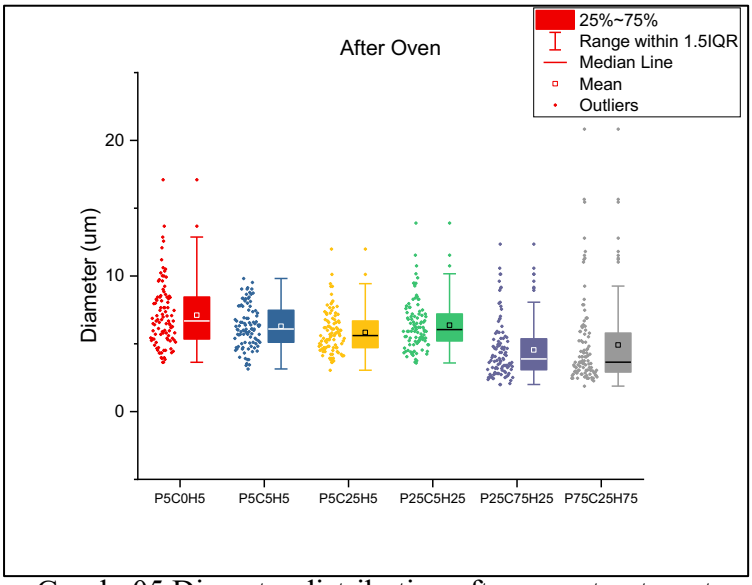

Graph. 05 Diameter distribution after oven treatment

After placing the solutions in the oven at 80°C for 24 hours, the average diameter of the droplets reduced in size to around 5 um. Although part of the solution was lost in the process and still the size of the drops is a little big for the size of the fibers, the procedure performed as expected and gave desired results.

5.5 Thermogravimetric Analysis (TGA)

5.5.1 By Method

The thermogravimetric analysis was done for every material. To compare the results, they were first compared by method, meaning that every material was compared with every method done for that material.

	Polymer
	CLCs
	DC
	IS-E
	Coaxial

Table 01 Graphic legend for TGA by method

Table 01 shows the legend of TGA graphs for Polymer, CLCs, and different methods In-Solution/Emulsion (IS-E), Dip Coating (DC), and Coaxial for Coaxial Forcespinning®.

The materials were analyzed to find the degradation temperature (Td), polymer residual mass (PRM), and final residual mass (FRM) of the materials. The data was compiled into a table like the one shown below for each material.

PVA TCLCs	Td (°C)	PRM (%)	FRM (%)
PVA	305.6	N/A	8.5
TCLCs	337.9	N/A	0.69
IS	434	14.22	3.05
DC	431.2	6.86	1.46

Table 02 TGA data of Polyvinyl Alcohol Thermochromic CLCs

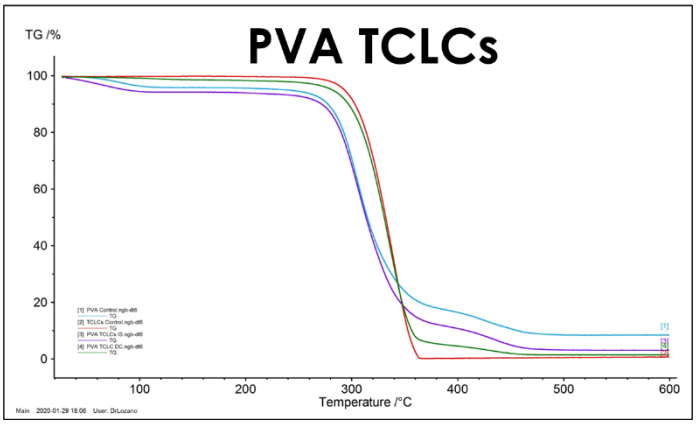

Graph. 06 TGA analysis of Polyvinyl Alcohol Thermochromic CLCs

Graph 06 and Table 02 show that Polyvinyl Alcohol has the lowest thermal stability once the polymer starts decomposing compared to the liquid crystal sample which has the highest one. Following this result, the composed samples reacted similarly with PVA In-Solution having lower thermal stability than that of the dip-coated one. It is important to notice that, due to the

nature of the process, the dip-coated sample has a higher concentration of liquid crystals with 93.14% than that of the In-Solution one with 85.78%.

PVA PCLCs	Td (°C)	PRM (%)	FRM (%)
PVA	305.6	N/A	8.5
PCLCs	320.1	N/A	0.86
IS	443.8	40.23	4.36
DC	436.9	13.62	1.68

Table 03 TGA data of Polyvinyl Alcohol Piezochromic CLCs

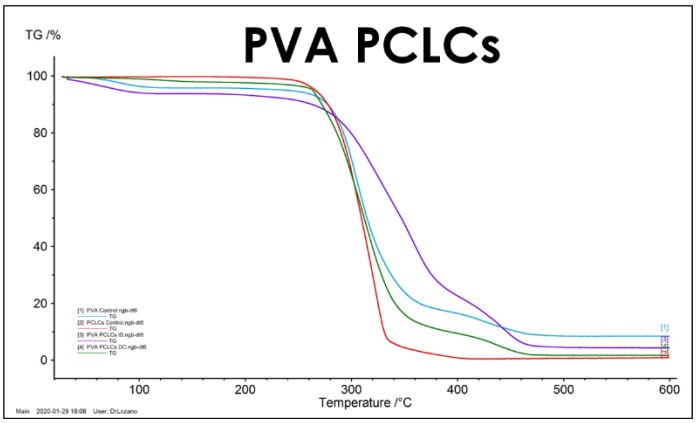

Graph. 07 TGA analysis of Polyvinyl Alcohol Piezochromic CLCs

Graph 07 shows similar behavior to that of graph 06, the lowest thermal stability is shown by PVA In-Solution, while the highest thermal stability is shown by the liquid crystal control sample. It is also important to notice that the degradation of the samples happens starts earlier for the samples with the highest concentration of liquid crystals than the ones with the lowest one. In this case PVA PCLC DC with 86.38% CLCs degrades at a faster rate than PVA PCLC IS with 59.77% CLCs.

PVA VOCs	Td (°C)	PRM (%)	FRM (%)
PVA	305.6	N/A	8.5
VOCs	343.5	N/A	2.66
DC	436.9	52.4	1.68

Table 04 TGA data of Polyvinyl Alcohol Piezochromic CLCs

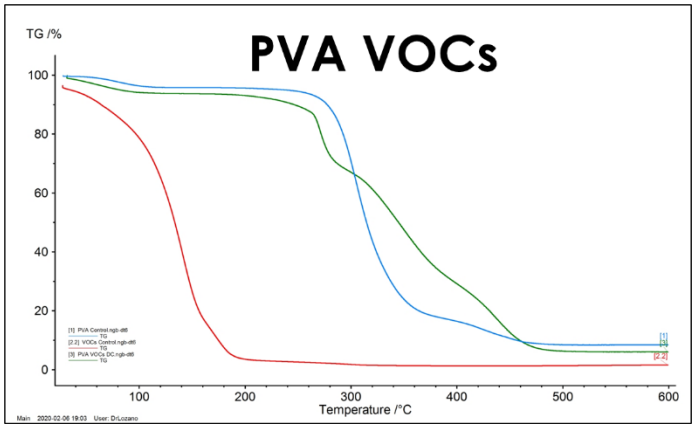

Graph. 08 TGA analysis of Polyvinyl Alcohol VOC CLCs

In graph 08 it can be seen that the PVA VOC sample has a higher affinity to PVA than with the VOC CLCs. The sample also shows an almost 50% polymer/CLC ratio. Something important to notice in this graph is that contrary to the previous ones PVA has higher thermal stability than the VOC CLCs.

PS TCLCs	Td (°C)	PRM (%)	FRM (%)
PS	413	N/A	0.2
TCLCs	337.9	N/A	0.69
IS	409.1	78.82	0.63
DC	422.8	15.58	0.26
Coaxial	409.1	80.16	-0.07

Table 05 TGA data of Polystyrene Thermochromic CLCs

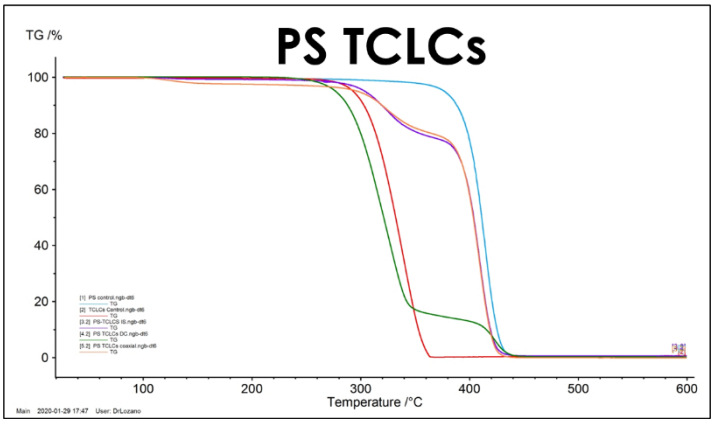

Graph. 09 TGA analysis of Polystyrene Thermochromic CLCs

As seen in graph 09 and table 05 Polystyrene has the highest thermal stability; on the other hand, the CLCs have low thermal stability and that affects the materials. PS TCLCs IS and PS TCLCs Coaxial have a similar behavior and as expected their degradation point is in between the polymer's and CLCs' thermal stability. The increment in thermal stability is due to the ~80% polymer in the material.

PS TCLCs DC, as expected, has 15.58% polymer due to the nature of the method having the polymer absorb part of the CLCs and drag some more on the surface. The singularity of this material is seen by its thermal stability being lower than that of the CLCs by themselves, this behavior may be explained by the amount of CLCs in the material and some other mechanical behavior present on the surface of the fibers. It is important to note that this analysis was done several times having the same result.

PS PCLCs	Td (°C)	PRM (%)	FRM (%)
PS	413	N/A	0.2
PCLCs	320.1	N/A	0.86
IS	419.6	81.9	0.75
DC	434.1	11.27	0.1
Coaxial	410.5	69.57	0.41

Table 06 TGA data of Polystyrene Piezochromic CLCs

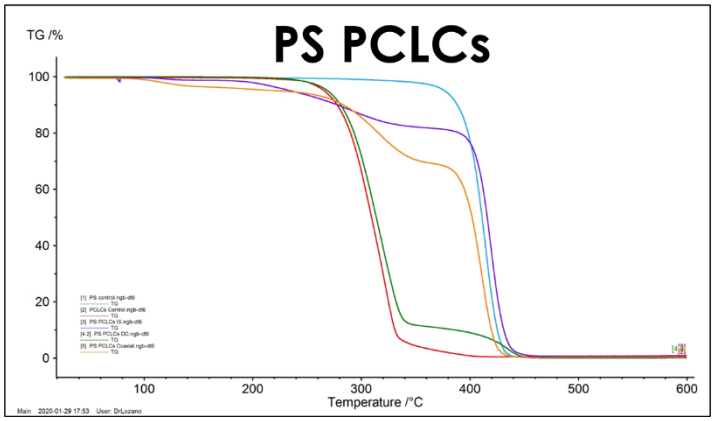

Graph. 10 TGA analysis of Polystyrene Piezochromic CLCs

As expected, graph 10 and table 06 show that the thermal stability of Polystyrene and the CLCs lay on both ends of the spectrum with the polymer having the highest thermal stability and the CLCs the lowest. All three other materials lay in between these ends with PS PCLCs IS and PS PCLCs Coaxial having a similar behavior at around ~20-30% CLCs and PS PCLCs DC at almost 90% CLCs.

PS VOCs	Td (°C)	PRM (%)	FRM (%)
PS	413	N/A	0.2
VOCs	343.5	N/A	2.66
IS	416.2	58.26	1.06
DC	410.6	12	0.45

Table 07 TGA data of Polystyrene VOC CLCs

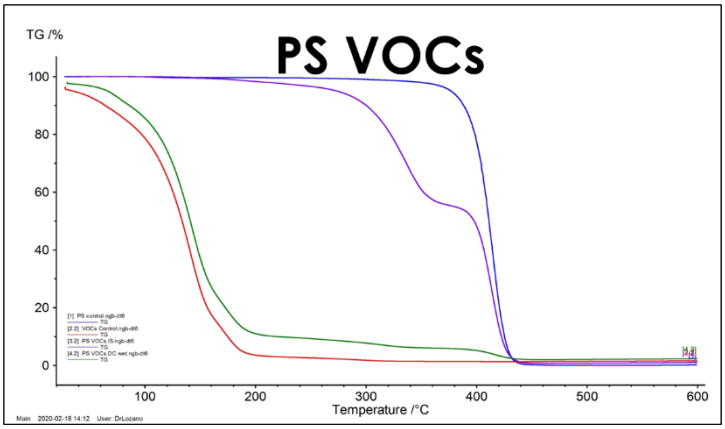

Graph. 11 TGA analysis of Polystyrene VOC CLCs

Graph 11 and Table 07 show the same behavior as the previous Polystyrene materials. The most excelling part of the results is the low thermal stability of the CLCs, as expected and seen in the graph, PS VOCs DC has more affinity towards the CLCs while PS VOCs IS has more affinity toward the polymer.

PEO PCLCs	Td (°C)	PRM (%)	FRM (%)
PEO	396.7	N/A	5.61
PCLCs	320.1	N/A	0.86
IS-E	392.7	64.15	2.66
DC	397.1	25.35	0.62

Table 08 TGA data of Polyethylene Oxide Piezochromic CLCs

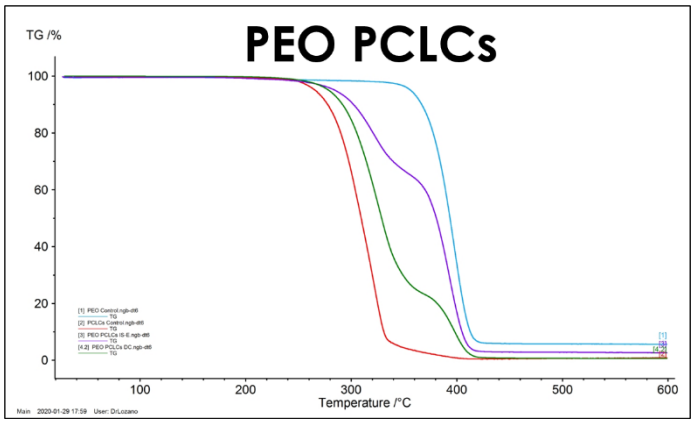

Graph. 12 TGA analysis of Polyethylene Oxide Piezochromic CLCs

Similar to Polystyrene results, graph 12 and table 08, show Polyethylene Oxide having the highest thermal stability and the CLCs the lowest one. PEO PCLCs IS-E shows a similar result as previous ones, having thermal stability closer to the polymer and a CLCs percentage of ~40. PEO PCLCs DC shows a similar result as well with the thermal stability closer to the CLCs and with a 25.35 polymer percentage.

PEO VOCs	Td (°C)	PRM (%)	FRM (%)
PEO	396.7	N/A	5.61
VOCs	343.5	N/A	2.66
DC	436.9	73.77	1.68

Table 09 TGA data of Polyethylene VOC CLCs

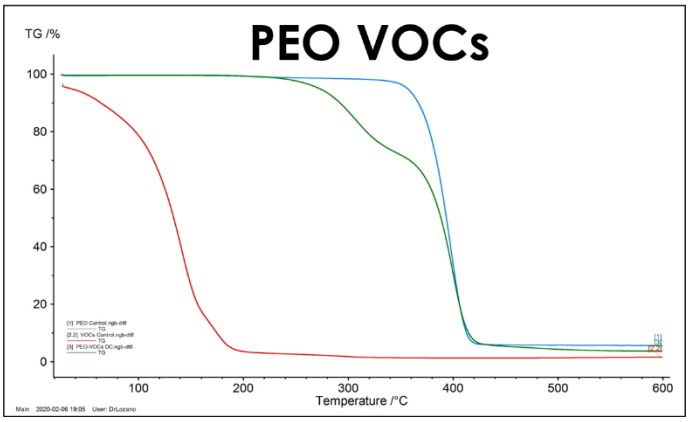

Graph. 13 TGA analysis of Polyethylene Oxide VOC CLCs

PEO VOCs DC has thermal stability between that of the polymer and the CLCs' with it being closer to the polymer's one and a 73.77 polymer percentage.

5.5.2 By Polymer

The second method of comparison was by polymer, meaning that all materials done with each polymer were compared together with the different CLCs and methods.

	Polymer
	TCLCs
	PCLCs
	VOCs
	Poly-TCLCs
	Poly-PCLCs
	Poly-VOCs

Table 10 Graphic legend for TGA by polymer

PS	Td (°C)	PRM (%)	FRM (%)
PS	413	N/A	0.2
TCLCs	337.9	N/A	0.69
PCLCs	320.1	N/A	0.86
VOCs	343.5	N/A	2.66
PS TCLCs DC	422.8	15.58	0.26
PS PCLCs DC	434.1	11.27	0.1
PS VOCs DC	410.6	94.26	0.45

Table 11 TGA data of Polystyrene

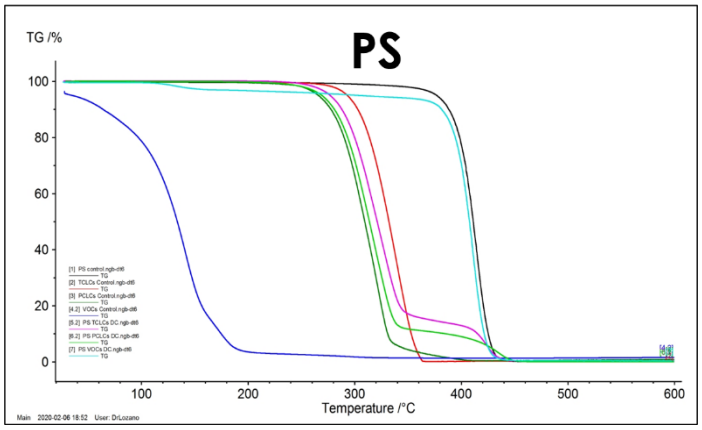

Graph. 14 TGA analysis of Polystyrene

After analyzing TGA by method, an analysis by polymer was done to compare the different methods and CLCs using the same material. Graph 14 shows an example of such a graph for PS samples, there were graphs done for PVA and PEO as well and placed in the appendix. These graphs were used as a summary of the graphs previously showed and how they all compared. Common in all by polymer graphs most of the composed samples fall in between the polymer control and CLC control. The composed samples also show similarities in the polymer/CLC ratios between methods.

5.6 Fourier-Transform Infrared Spectroscopy (FTIR)

5.6.1 By CLCs

An FTIR spectroscopy was performed for all materials; for CLCs the FTIR spectroscopy was done to prove that the components are present in the final solution of CLCs.

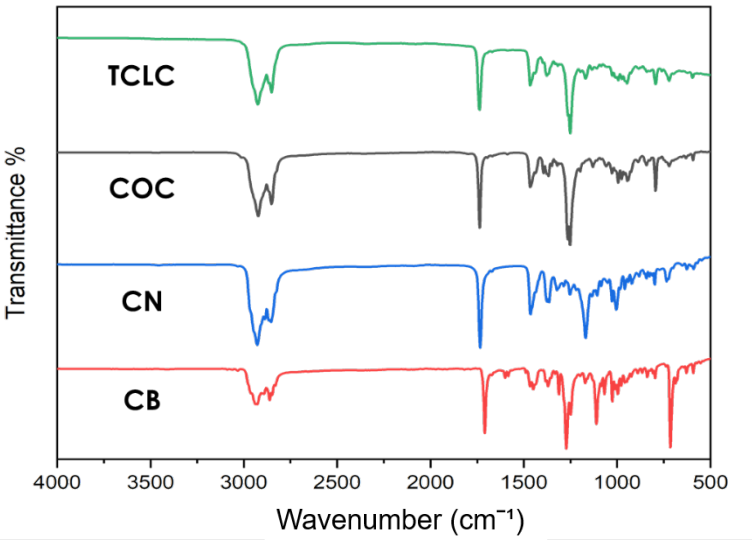

Graph. 15 FTIR of Thermochromic CLCs

Thermochromic CLCs are composed of three different CLCs, Cholesteryl Oleyl Carbonate (COC), Cholesteryl Nonanoate (CN), and Cholesteryl Benzoate (CB) with solution percentages of 65, 25 and 10, respectively. An FTIR spectroscopy was performed for all the components and then compiled into a single plot to compare against the final solution.

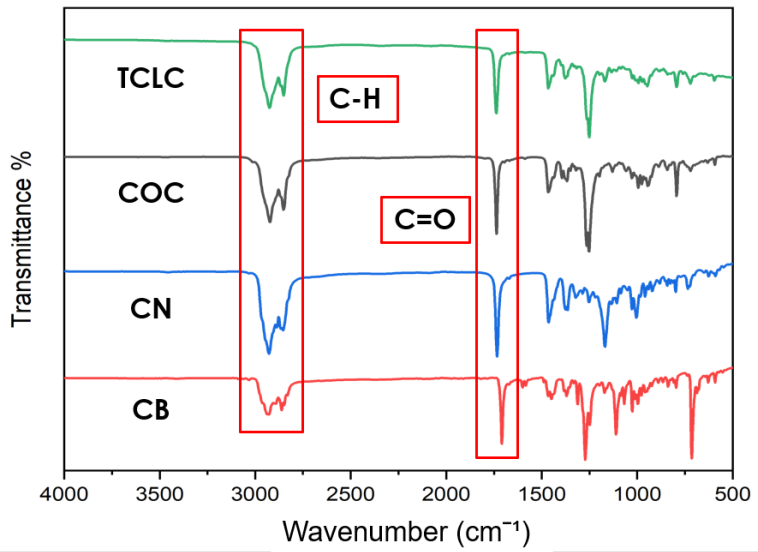

Graph. 16 FTIR analysis of Thermochromic CLCs

The FTIR spectrum was analyzed and compared against their molecular structure. The carbon-hydrogen bond was identified as well as the carbonyl molecule, as seen in graph 16.

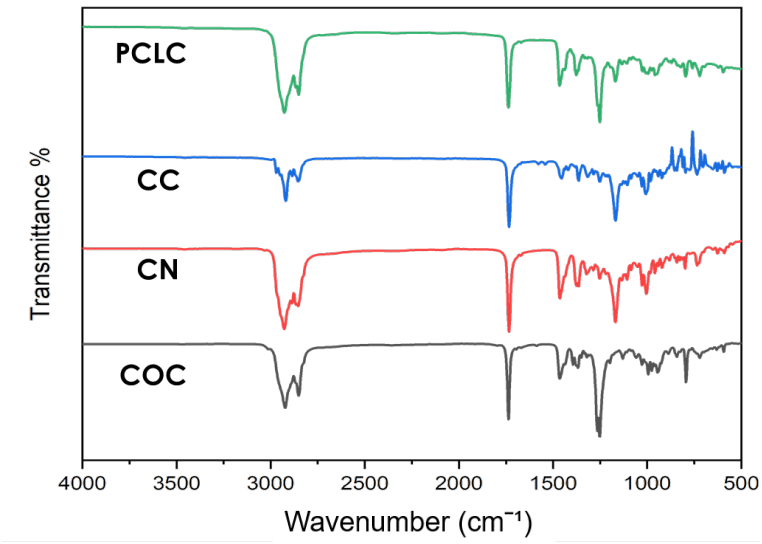

Graph. 17 FTIR of Piezochromic CLCs

Piezochromic CLCs have a different composition than that of the TCLCs even though it still has COC and CN, it replaces its last component for Cholesteryl Chloride (CC). The difference also lays in the component percentages in the solution having 38% COC, 38% CN, and 25% CC.

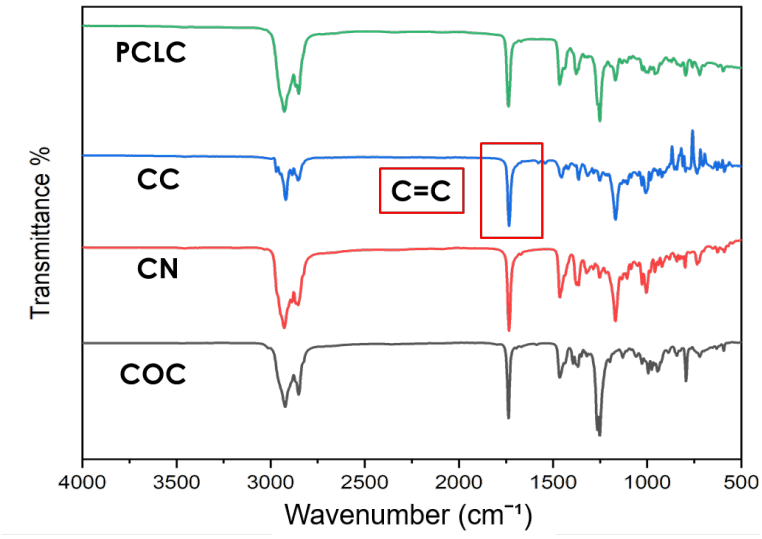

Graph. 18 FTIR analysis of Piezochromic CLCs

FTIR analysis was also performed and the same carbon-hydrogen bond was identified, it appears to have the same carbonyl as well but comparing the FTIR to the molecular structure of the new component, it was discovered that there was no carbon-oxygen bond. Although there was a carbon=carbon double bond present in the structure, therefore it was concluded that the peak shown at around 1750 cm^{-1} is the carbon=carbon double bond and not the carbonyl shown in the other components.

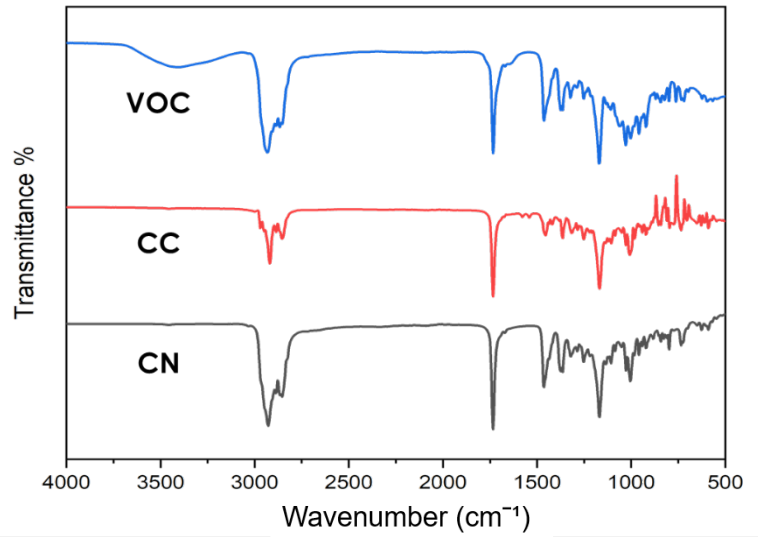

Graph. 19 FTIR spectroscopy of VOC CLCs

CLCs to detect volatile organic components were also analyzed, although by using the same components as the previous CLCs, there is no discussion about what the peaks at around 1750 cm^{-1} and 3000 cm^{-1} are. The only thing to notice in this spectrum is the bump shown at 3500 cm^{-1}, which was identified to be the Tetrahydrofuran present in the solution.

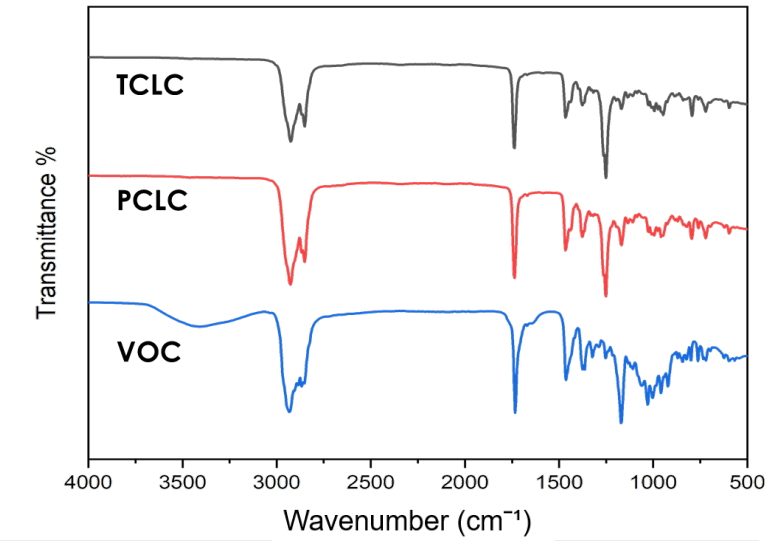

Graph. 20 FTIR comparison of CLCs

Graph 20 is a comparison of all three CLCs, they look very similar between each other except for a few things that were previously discussed.

5.6.2 By Polymer

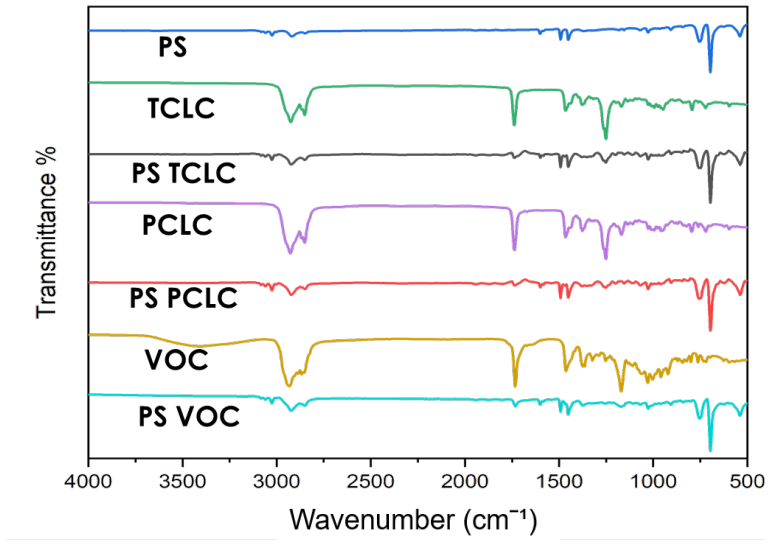

Graph. 21 FTIR of Polystyrene materials

The FTIR spectroscopy graphs by polymer were used to compare all composed samples from each polymer. By doing this comparison the similarities and determination of the components are easily identifiable. The graphs were arranged in a way so that the composed samples were placed below their respective CLCs. Graph 24 is one of the two graphs made, the graph for PVA can be seen in the appendix.

5.7 Differential Scanning Calorimetry (DSC)

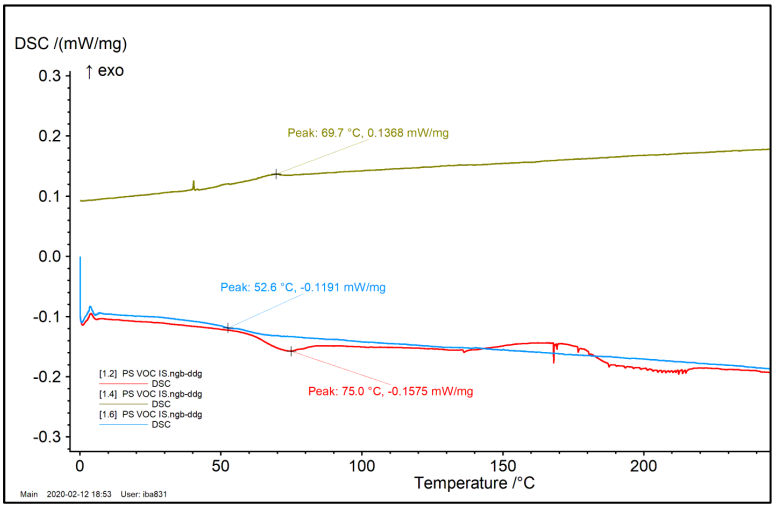

Graph. 22 DSC of PS VOC IS sample

Graph. 24 is one of the DSC graphs made for each sample. The importance of these DSC graphs is the information gathered, like processing information from the original batch and analysis of material behavior under a controlled environment. In graph 24, the red curve represents the processing induced thermal structure, the green curve is the crystallization of the material, which erases the processing properties induced at fabrication, and finally, the blue curve shows the intrinsic properties of the system. By analyzing the behavior of the material throughout the experiment the first melting point can be seen between 60°C and 85°C, later a meso order cold crystallization is present between 150°C and 180°C followed right after by a melting.

CHAPTER VI

CONCLUSION & FUTURE WORK

6.1 Conclusion

In conclusion, CLCs are a smart material with great potential for many applications including sensors. The three CLCs properties that are discussed in this investigation are thermochromism, piezochromism, and sensing of volatile organic components. Four different methods are being implemented in this research; the in-solution method, which resulted in not being a viable solution for the project unless it was implemented using PEO, which in that case it would emulate the emulsion method. The dip-coating method showed really good results for the functional part of the CLCs, but it still kept the problem of handling the CLCs. Therefore, even though the dip-coating had a matrix to hold on to, it still needed a film on top to be manipulated without leaving residue or wear away the material. The coaxial spinning method on the other hand, is the most promising one in this project since it has been proven that the optical properties can be seen and no film is needed. The main difficulty right now is the stability of the spinneret and the not so perfect aligning of the coaxial fibers, which leads to bleeding of the inner material, mostly for liquids. The final method, the emulsion method is also very promising but it needs to be optimized and further investigation needs to be conducted.

6.2 Future Work

- The coaxial spinneret is constantly being updated depending on the performances.
- Emulsion method is still in progress of being optimized using different techniques for either make the fibers larger or the drops smaller.

REFERENCES

[1] Aguilar, M.r., and J. San Román. “Introduction to Smart Polymers and Their Applications.” *Smart Polymers and Their Applications*, 2014, pp. 1–11., doi:10.1533/9780857097026.1.

[2] Lu, Yuan, *et al*. “Functional Transparent Nanocomposite Film with Thermochromic and Hydrophobic Properties Fabricated by Electrospinning and Hot-Pressing Approach.” *Ceramics International*, vol. 44, no. 1, 2018, pp. 1013–1018., doi:10.1016/j.ceramint.2017.10.037.

[3] Geng, Xiaoye, *et al*. “Reversible Thermochromic Microencapsulated Phase Change Materials for Thermal Energy Storage Application in Thermal Protective Clothing.” *Applied Energy*, vol. 217, 2018, pp. 281–294., doi:10.1016/j.apenergy.2018.02.150.

[4] Hu, J., and J. Lu. “Smart Polymers for Textile Applications.” *Smart Polymers and Their Applications*, 2014, pp. 437–475., doi:10.1533/9780857097026.2.437.

[5] Roy, Ipsita, and Munishwar Nath Gupta. “Smart Polymeric Materials.” *Chemistry & Biology*, vol. 10, no. 12, 2003, pp. 1161–1171., doi:10.1016/j.chembiol.2003.12.004.

[6] James, Honey Priya, *et al.* “Smart Polymers for the Controlled Delivery of Drugs – a Concise Overview.” *Acta Pharmaceutica Sinica B*, vol. 4, no. 2, 2014, pp. 120–127., doi:10.1016/j.apsb.2014.02.005.

[7] Mulder, D. J., *et al.* “Chiral-Nematic Liquid Crystals as One Dimensional Photonic Materials in Optical Sensors.” *J. Mater. Chem. C*, vol. 2, no. 33, 2014, pp. 6695–6705., doi:10.1039/c4tc00785a.

[8] Yang, Haiyue, *et al*. “Composite Phase Change Materials with Good Reversible Thermochromic Ability in Delignified Wood Substrate for Thermal Energy Storage.” *Applied Energy*, vol. 212, 2018, pp. 455–464., doi:10.1016/j.apenergy.2017.12.006.

[9] Panák, Ondrej, *et al*. “Insight into the Evaluation of Colour Changes of Leuco Dye Based Thermochromic Systems as a Function of Temperature.” *Dyes and Pigments*, vol. 120, 2015, pp. 279–287., doi:10.1016/j.dyepig.2015.04.022.

[10] Andrienko, Denis. “Introduction to Liquid Crystals.” *Journal of Molecular Liquids*, vol. 267, 2018, pp. 520–541., doi:10.1016/j.molliq.2018.01.17

[11] Jin, Yang, *et al.* "Preparation and Luminescence Studies of Thermosensitive PAN Luminous Fiber Based on the Heat Sensitive Rose Red TF-R1 Thermochromic Pigment." *Dyes and Pigments*, vol. 139, 2017, pp. 693–700., doi:10.1016/j.dyepig.2017.01.003.

[12] Jin, Yang, *et al*. "Thermosensitive Luminous Fiber Based on Reversible Thermochromic Crystal Violet Lactone Pigment." *Dyes and Pigments*, vol. 146, 2017, pp. 567–575., doi:10.1016/j.dyepig.2017.07.062.

[13] Bao, Suping, *et al*. "Reversible Thermochromic Switching of Fluorescent Poly(Vinylidene Fluoride) Composite Containing Bis(Benzoxazolyl)Stilbene Dye." *Dyes and Pigments*, vol. 99, no. 1, 2013, pp. 99–104., doi:10.1016/j.dyepig.2013.04.005.

[14] Lin, Pengcheng, *et al*. "Electrically Modulated Optical Properties of Fluorescent Chiral Nematic Liquid Crystals." *Chemical Engineering Journal*, vol. 341, 2018, pp. 565–577., doi:10.1016/j.cej.2018.02.007.

[15] Kulčar, Rahela, *et al*. "Colorimetric Properties of Reversible Thermochromic Printing Inks." *Dyes and Pigments*, vol. 86, no. 3, 2010, pp. 271–277., doi:10.1016/j.dyepig.2010.01.014.

[16] Malherbe, Ilana, *et al.* "Reversibly Thermochromic Micro-Fibres by Coaxial Electrospinning." *Polymer*, vol. 51, no. 22, 2010, pp. 5037–5043., doi:10.1016/j.polymer.2010.09.018.

[17] Martinez-Hurtado, Juan L. "Elastic Holograms." *DIVERSE ENGAGEMENT: DRAWING IN THE MARGINS*, 28 June 2010, pp. 113–117.

[18] Leclerc *et al*., "Optical and Electrochemical Transducers Based on Functionalized Conjugated Polymers"**,** 1999, *Advanced Materials,* **11,** 18, 1491-1498

[19] Song *et al.,* "Studies of Chain Conformational Kinetics in Poly(di-n-alkylsilanes). 5. The Effect of Side-Chanin Structure on Piezochromism", 1992, *Macromolecules*, **25,** 3629-3632

[20] Zhang, Rong; Cai, Weizhao; Bi, Tiange; Zarifi, Niloofar; Terpstra, Tyson; Zhang, Chuang; Verdeny, Z. Valy; Zurek, Eva; Deemyad, Shanti (2017). "Effects of Nonhydrostatic Stress on Structural and Optoelectronic Properties of Methylammonium Lead Bromide Perovskite". *The Journal of Physical Chemistry Letters*. 8 (15): 3457–3465.

[21] Cai, Weizhao; Zhang, Rong; Yao, Yansun; Deemyad, Shanti (2017). "Piezochromism and structural and electronic properties of benz[a]anthracene under pressure". *Phys. Chem. Chem. Phys*. 19 (8): 6216–6223.

[22] Burgess *et al*, "Solvent effects on piezochromism of transition metal complexes", 1998, *Transition metal Chemistry.,* 23, 615-618

[23] Etaiw *et al*., "Unusual behaviour of the solid supramolecular 3D polymers $[(Me_3Sn)_nFe(CN)_6]$¥ (n=3/4)", 1996, *Journal of Organometallic Chemistry,* 522, 77-86

[24] Zharkova, G. M., *et al*. "Optical Polymer Liquid Crystal Pressure Sensors." *PROCEEDINGS OF THE XXV CONFERENCE ON HIGH-ENERGY PROCESSES IN CONDENSED MATTER (HEPCM 2017)*, Oct. 2017, doi:10.1063/1.5007459.

[25] Kottapalli, A G P, *et al.* "A Flexible Liquid Crystal Polymer MEMS Pressure Sensor Array for Fish-like Underwater Sensing." *Smart Materials and Structures*, vol. 21, no. 11, 23 October 2012, p. 115030., doi:10.1088/0964-1726/21/11/115030.

[26] Wolkoff, P.; Wilkins, C. K.; Clausen, P. A.; Nielsen, G. D. (2006). "Organic compounds in office environments - sensory irritation, odor, measurements and the role of reactive chemistry". Indoor Air. **16** (1): 7–19.

[27] "Volatile Organic Compounds' Impact on Indoor Air Quality." *EPA*, Environmental Protection Agency, 6 Nov. 2017, www.epa.gov/indoor-air-quality-iaq/volatile-organic-compounds-impact-indoor-air-quality.

[28] Wang, Junren, *et al*. "Liquid Crystal/Polymer Fiber Mats as Sensitive Chemical Sensors." *Journal of Molecular Liquids*, vol. 267, 2018, pp. 490–495., doi:10.1016/j.molliq.2018.01.051.

[29] Han, Yang, *et al.* "Optical Monitoring of Gases with Cholesteric Liquid Crystals." *JACS*, vol. 132, no. 9, 15 Sept. 2009, pp. 2961–2967., doi:JA907826Z.

[30] Mujahid, Adnan, *et al*. "Solvent Vapour Detection with Cholesteric Liquid Crystals—Optical and Mass-Sensitive Evaluation of the Sensor Mechanism." *Sensors*, vol. 10, no. 5, 2010, pp. 4887–4897., doi:10.3390/s100504887.

[31] Tang, Jieyuan, *et al.* "All-Fiber-Optic VOC Gas Sensor Based on Side-Polished Fiber Wavelength Selectively Coupled with Cholesteric Liquid Crystal Film." *Sensors and Actuators B: Chemical*, vol. 273, 2018, pp. 1816–1826., doi:10.1016/j.snb.2018.06.105.

[32] Winterbottom, Daniel A., *et al*. "Cholesteric Liquid Crystals for Detection of Organic Vapours." *Sensors and Actuators B: Chemical*, vol. 90, no. 1-3, 2003, pp. 52–57., doi:10.1016/s0925-4005(03)00021-2.

[33] Reinitzer, Friedrich. "Beiträge Zur Kenntniss Des Cholesterins." *Monatshefte Für Chemie - Chemical Monthly*, Springer-Verlag, 1 Dec. 1888.

[34] "History and Properties of Liquid Crystals." *Liquid Crystals Nobel*, Beloit College, 9 Sept. 2003, chemistry.beloit.edu/classes/nanotech/LC/liquid_crystals_nobel.pdf.

[35] Russell, Joette M., *et al*. "Alignment of Nematic Liquid Crystals Using Carbon Nanotube Films." *Thin Solid Films*, vol. 509, no. 1-2, 12 Oct. 2005, pp. 53–57., doi:10.1016/j.tsf.2005.09.099.

[36] Rahman, Md. Asiqur, *et al.* "Incorporation and Orientational Order of Aligned Carbon Nanotube Sheets on Polymer Films for Liquid Crystal-Aligning Transparent Electrodes." *Journal of Molecular Liquids*, vol. 267, 2018, pp. 363–366., doi:10.1016/j.molliq.2017.12.122.

[37] Fu, Weiqi, *et al*. "Super-Aligned Carbon Nanotube Films as Aligning Layers and Transparent Electrodes for Liquid Crystal Displays." *Carbon*, vol. 48, no. 7, 2010, pp. 1876–1879., doi:10.1016/j.carbon.2010.01.026.

[38] Serra, Francesca, *et al.* "The Emergence of Memory in Liquid Crystals." *Materials Today*, vol. 14, no. 10, 2011, pp. 488–494., doi:10.1016/s1369-7021(11)70213-9.

[39] Lagerwall, Jan P.f., and Giusy Scalia. "A New Era for Liquid Crystal Research: Applications of Liquid Crystals in Soft Matter Nano-, Bio- and Microtechnology." *Current Applied Physics*, vol. 12, no. 6, 2012, pp. 1387–1412., doi:10.1016/j.cap.2012.03.019.

[40] Dowden, W.a. "Cholesteric Liquid Crystals-A Review of Developments and Applications." *Non-Destructive Testing*, vol. 1, no. 2, 1967, pp. 99–102., doi:10.1016/0029-1021(67)90029-1.

[41] Sarkar, K., *et al*., "Electrospinning to Forcespinning™". Materials Today, 2010. 13(11): p. 12- 14.

[42] Lozano, K. and Sarkar, K., *Methods and apparatuses for making superfine fibers*, US20090280325 A1.

[43] Lozano, K. and Sarkar, K., *Superfine fiber creating spinneret and uses thereof*, US20090280207 A1.

[44] Nakata, Masahiro, *et al*. "Hollow Fibers Containing Various Display Elements: A Novel Structure for Electronic Paper." *Journal of the Society for Information Display*, vol. 14, no. 8, 2006, p. 723., doi:10.1889/1.2336099.

[45] Lagerwall, Jan P. F., *et al.* "Coaxial Electrospinning of Microfibres with Liquid Crystal in the Core." *Chemical Communications*, no. 42, 2008, p. 5420., doi:10.1039/b810450f.

[46] Enz, Eva, and Jan Lagerwall. "Electrospun Microfibres with Temperature Sensitive Iridescence from Encapsulated Cholesteric Liquid Crystal." *Journal of Materials Chemistry*, vol. 20, no. 33, 2010, p. 6866., doi:10.1039/c0jm01223h.

[47] Buyuktanir, Ebru A., *et al*. "Self-Assembled, Optically Responsive Nematic Liquid Crystal/Polymer Core-Shell Fibers: Formation and Characterization." *Polymer*, vol. 51, no. 21, 2010, pp. 4823–4830., doi:10.1016/j.polymer.2010.08.011.

[48] Guan, Yu, *et al.* "Preparation of Temperature-Response Fibers with Cholesteric Liquid Crystal Dispersion." *Colloids and Surfaces A: Physicochemical and Engineering Aspects*, vol. 546, 2018, pp. 212–220., doi:10.1016/j.colsurfa.2018.03.011.

[49] Guan, Yu, *et al.* "Preparation of Thermochromic Liquid Crystal Microcapsules for Intelligent Functional Fiber." *Materials & Design*, vol. 147, 2018, pp. 28–34., doi:10.1016/j.matdes.2018.03.030.

[50] Barbero, Giovanni, *et al*. "Twist Transitions and Force Generation in Cholesteric Liquid Crystal Films." *Journal of Molecular Liquids*, vol. 267, 2018, pp. 242–248., doi:10.1016/j.molliq.2017.11.014.

[51] Matsuyama, Akihiko. "Theory of Polymer-Dispersed Cholesteric Liquid Crystals." *The Journal of Chemical Physics*, vol. 139, no. 17, 2013, p. 174906., doi:10.1063/1.4828940.

[52] Ahmad, Farzana, *et al.* "Study of Polymer Dispersed Liquid Crystal Film Based on Amphiphilic Polymer Matrix." *Arabian Journal of Chemistry*, vol. 10, 2017, doi:10.1016/j.arabjc.2014.01.022.

[53] Yan, Qi, *et al*. "Polymer Stabilized Cholesteric Liquid Crystal Particles with High Thermal Stability." *Optical Materials Express*, vol. 8, no. 6, 2018, p. 1536., doi:10.1364/ome.8.001536.

[54] Katz, David A. "Preparation of Cholesteryl Ester Liquid Crystals." *Pima Community College*, 2011.

[55] G. H. Brown and J. J. Wolken, *Liquid Crystals and Biological Systems*, Academic Press, NY, 1979, pp. 165-167

[56] W. Elser and R. D. Ennulat, *Adv. Liq. Cryst.* 2, 73 (1976)

[57] Patch, Graeme, and Gregory A. Hope. "Preparation and Properties of Cholesteric Liquid Crystals." *Journal of Chemical Education*, vol. 62, no. 5, 1985, p. 454., doi:10.1021/ed062p454.

[58] "TA INSTRUMENTS DIFFERENTIAL SCANNING CALORIMETER (DSC)." *TQ100 Operating Instructions*, faculty.olin.edu/~jstolk/matsci/Operating%20Instructions/DSC%20Operating%20Instructions.pdf.

[59] Zhou, Hui, et al. “A Novel Method for Kinetics Analysis of Pyrolysis of Hemicellulose, Cellulose, and Lignin in TGA and Macro-TGA.” *RSC Advances*, vol. 5, no. 34, 2015, pp. 26509–26516., doi:10.1039/c5ra02715b.

[60] Mohamed, M.A., et al., Chapter 1 - Fourier Transform Infrared (FTIR) Spectroscopy, in Membrane Characterization, N. Hilal, et al., Editors. 2017, Elsevier. p. 3-29.

[61] Mukhopadhyay, Ankan. “MEASUREMENT OF MAGNETIC HYSTERESIS LOOPS IN CONTINUOUS AND PATTERNED FERROMAGNETIC NANOSTRUCTURES BY STATIC MAGNETO-OPTICAL KERR EFFECT MAGNETOMETER.” *SNBNCBS*, July 2015.

[62] “TEVO Tornado - TEVO 3D Printers & Kits: TEVO 3D Electronic Limited.” *TEVO 3D Printers & Kits | TEVO 3D Electronic Limited*, 14 Aug. 2019, www.tevo.cn/products/3d-printers/tevo-tornado/.

[63] “Microscopy.” *Microscopy*, www.sussexvt.k12.de.us/science/cell%20structure%20and%20function/microscopy.htm.

APPENDIX A

APPENDIX A

1A. TGA by Polymer

PVA	Td (°C)	PRM (%)	FRM (%)
PVA	305.6	N/A	8.5
TCLCs	337.9	N/A	0.69
PCLCs	320.1	N/A	0.86
VOCs	343.5	N/A	2.66
PVA TCLCs DC	431.2	6.86	1.46
PVA PCLCs DC	436.9	13.62	1.68
PVA VOCs DC	437.3	52.4	6.06

Table A1 TGA data of Polyvinyl Alcohol

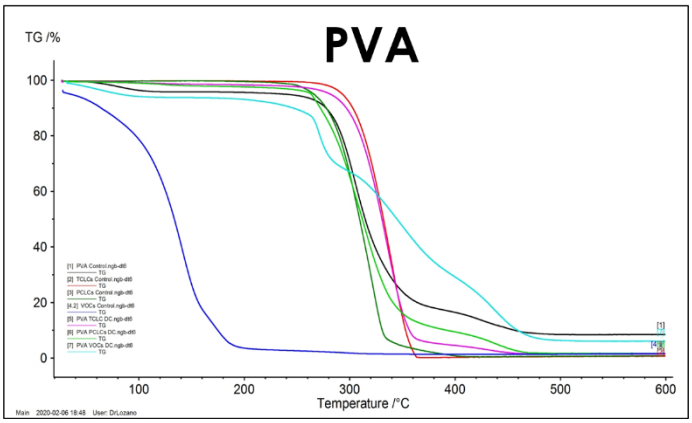

Graph. A1 TGA analysis of Polyvinyl Alcohol

PEO	Td (°C)	PRM (%)	FRM (%)
PEO	396.7	N/A	5.61
TCLCs	337.9	N/A	0.69
PCLCs	320.1	N/A	0.86
VOCs	343.5	N/A	2.66
PEO TCLCs DC	395.4	36.84	1.56
PEO PCLCs DC	397.1	25.35	0.62
PEO VOCs DC	399.9	73.77	3.7

Table A2 TGA data of Polyethylene Oxide

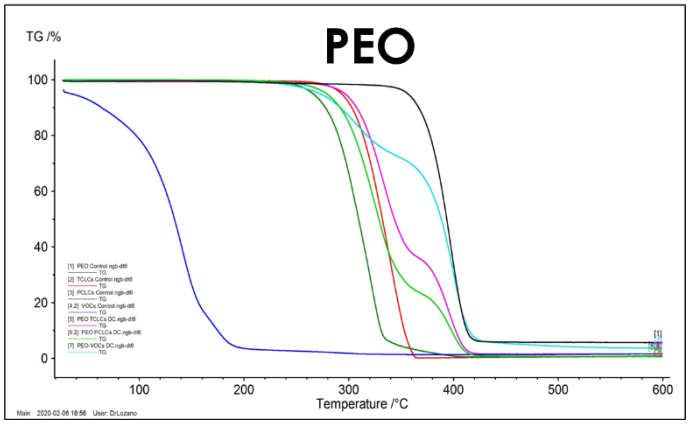

Graph. A2 TGA analysis of Polyethylene Oxide

2A. FTIR by Polymer

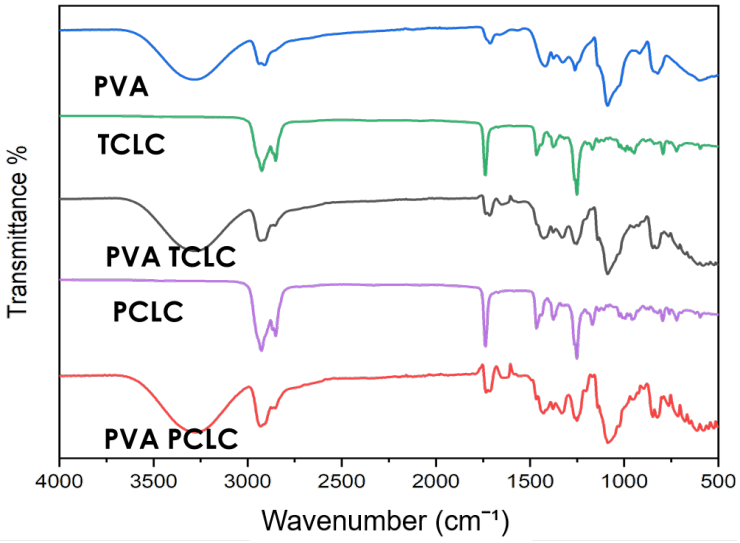

Graph. A3 FTIR of Polyvinyl Alcohol materials

2A. State-of-the-Art Tables

Equipment	Purpose	Results Obtained
SEM	Microscope to see morphology of the fibers	Fibers with CLCs did not change the morphology of the fibers
DSC	Measures transition temperature and heat flow	Graphs of CLCs, fibers, polymeric materials and a combination of the three were used to obtain data about their processing and behavior towards temperature changes
TGA	Measures weight changes	Used to understand the thermal stability of the materials and identify their degradation point as well as the CLCs to polymer ratio.
Forcespinning	Production of nanofibers	A good amount of samples were obtain. These samples were either characterized as they came out or further treatment was done. Resulting fibers gave a mix of positive and negative results through the methods used.
Homogenizer	Mixing of a solution's components in order to have a homogeneous solution	Used mostly during the Emulsion method to have a homogenious solution as well as small CLC droplets.
FTIR	Obtain an infrared spectrum of absorption or emission of a solid, liquid, or gas.	Used to find the element composition of a sample and chemical bonding. As well as to compare their components in order to make sure they are still present in the final product.
3D printer	3-D print	Make a coaxial spinneret

Table A3 State-of-the-Art Equipment

Equipment	Purpose	Results Obtained
Solidworks	CAD program to creat 3D models	The program was used to create a coaxial spinneret
TA Universal Analysis	Analyze data from TGA and DSC	Found melting point for materials, (double melting point for CLCs) - XPS, degradation point of materials -TGA.
Image J	Image analysis program	Used to analyze images from optical microscopes and SEM. Specifically diameter analysis of nanofibers made by Forcespinning and droplets from emulsions made.

Table A4 State-of-the-Art Software

BIOGRAPHICAL SKETCH

Ydana Y. Virgen Gracia, ydana.virgen@gmail.com, was born in Reynosa, Tamaulipas, Mexico. She completed a Bachelor of Science in Mechanical Engineering at the University of Texas Rio Grande Valley in December 2017.

In the Fall of 2017, she was accepted to the University of Texas Rio Grande Valley Mechanical Engineering Graduate Program, where she began working as a Graduate Research Assistant for Dr. Karen Lozano. During her time, she worked in projects such as the wettability of some hydrophobic materials, a fog catcher using nanotechnology, and cholesteric liquid crystals as sensors.

She completed and defended her thesis to attain her Master's degree in Mechanical Engineering from the University of Texas Rio Grande Valley in February 2020. Later that year, in July 2020 she graduated with a Master's degree in Mechanical Engineering from the University of Texas Rio Grande Valley.